Using antibody synergy to engineer a high potency biologic cocktail against *C. difficile*

Hui Zhao[1], Michael Tasch[1], Michael Dodds[1], Mesfin Gewe[1], Anissa Martinez[1], Melanie Hutton[2], Kristie Keeney[1], Alex Pollock[1], Ben Jester[1], Nhi Khuong[1], Mia Zhang[1], Colin Brady[1], Mark Heinnickel[1], Hannah Tabakh[1], Nathan Sanjaya[1], Kendra Cruickshank[1], Troy Paddock[1], Stacey Ertel[1], Sarah Struyvenberg[1], Jason Dang[1], Tracy Saveria[1], Chelsea Shanitta[1], David Fletcher[1], Lauren Goetsch[1], Caitlin Gamble[1], Steven J. Mileto[2], Ryan Heselpoth[3], Dena Lyras[2], Craig A. Behnke[1], Vincent Fischetti[3], Brian Finrow[1], and James M. Roberts[1,4]

[1]Lumen Bioscience, Seattle, WA
[2]Biomedicine Discovery Institute and Department of Microbiology, Monash University, Victoria, Australia
[3]Laboratory of Bacterial Pathogenesis and Immunity, Rockefeller University, New York, NY
[4]Corresponding author: James M. Roberts, Lumen Bioscience, 1441 N. 34th Street, Seattle, WA, 98103, jroberts@lumen.bio

Keywords: *Arthrospira platensis*; spirulina; *C. difficile*; VHH; lysin; oral therapeutic; synergy

ABSTRACT

We applied a mathematical framework originally used to model the effects of multiple inhibitors on enzyme activity to guide the development a therapeutic antibody cocktail, LMN-201, to prevent and treat *C. difficile* infection (CDI). CDI causes hundreds of thousands of cases of severe, often recurrent diarrhea and colitis in the United States annually and is associated with significant morbidity and mortality worldwide. Current therapies for preventing recurrent CDI are only partially successful, and there are no options available to prevent initial bouts of CDI in at-risk populations. Almost all antibody therapies have been developed and administered as monotherapies. Antibody cocktails are relatively rare even though they have the potential to greatly increase efficacy. One reason for this is our limited understanding of how antibody interactions can enhance potency, which makes it difficult to identify and develop antibodies that can be assembled into optimally effective cocktails. In contrast to the view that antibody synergies depend on unusual instances of cooperativity or allostery, we show that synergistic efficacy requires nothing more than that the antibodies bind independently to distinct epitopes on a common target. Therefore, synergy may be achieved much more readily than is generally appreciated. Due to synergy the LMN-201 antibody cocktail, which targets the *C. difficile* exotoxin B (TcdB), is 300- to 3000-fold more potent at neutralizing the most clinically prevalent TcdB toxin types than bezlotoxumab, the only monoclonal antibody currently approved for treatment or prevention of CDI. The efficacy of LMN-201 is further enhanced by inclusion of a phage-derived endolysin that destroys the C. difficile bacterium, and which therefore has a complementary mechanism of action to the antibody cocktail. These observations may serve as

42 a paradigm for the development of high potency biologic cocktails against targets that have

43 proven challenging for single-agent therapies.

44

45

46 **INTRODUCTION**

47 *Clostridioides difficile* is a Gram-positive spore-forming anaerobic bacterium[1]. *C. difficile*
48 infection (CDI) causes severe, recurrent diarrhea and colitis and is associated with significant
49 morbidity and mortality world-wide[2]. According to the U.S. Centers for Disease Control and
50 Prevention, *C. difficile* is the most common cause of health care-associated infections in U.S
51 hospitals, where nearly half a million CDI cases occur each year[3]. Though traditionally
52 considered a nosocomial infection, community-associated CDI is on the rise and now comprises
53 most cases in some regions[4]. Treatment costs are estimated to exceed $5 billion a year, but the
54 true economic burden of the disease is far higher when lost quality-adjusted life years are
55 considered[4].

56 *C. difficile* virulence is mediated by expression of two homologous, multidomain exotoxins,
57 TcdA and TcdB[5–8]. The toxins initially engage cell surface receptors on intestine epithelial cells,
58 which results in internalization by endocytosis[9,10]. Acidification of internalized endosomes
59 triggers a conformational change in the toxin that promotes its translocation into the
60 cytoplasm[11]. Cytoplasmic toxin undergoes autoproteolysis[12], releasing its N-terminal
61 glucosyltransferase domain that enzymatically inhibits Rho family-GTPases by mono-
62 glucosylation[13,14]. Inactivation of Rho disaggregates the cellular actin cytoskeleton thereby
63 disrupting the colonic epithelium[15–17], leading to severe inflammation and watery diarrhea
64 characteristic of CDI. The relative importance of TcdA and TcdB for causing *C. difficile* pathology
65 varies by host species, and current balance of opinion is that human pathophysiology is
66 primarily caused by TcdB[7,18–23].

67 Antibiotic therapy is often successful for initial cases of CDI. However, approximately 20%-40%
68 of CDI patients will have a recurrent episode[24], and the chance of additional episodes in those
69 patients exceeds 40%[25,26]. Microbial dysbiosis is a consequence of the antibiotics most often
70 used to treat CDI, which creates a niche favorable to *C. difficile* proliferation[27] and promotes
71 recurrent disease. Due to side effects and selection for antimicrobial resistance, antibiotics are
72 no longer used prophylactically.

73 One alternative to antibiotics for treatment of microbial pathogens is passive immunization by
74 direct infusion of neutralizing antibodies. Intravenous or intraperitoneal infusion of monoclonal
75 and polyclonal antibodies targeting TcdA and TcdB are protective against primary infection and
76 relapse in *C. difficile* challenge models in mice[8,21,28,29], hamsters,[30,31] piglets[22,32]. It is important
77 that immunotherapies used clinically address the natural antigenic variation displayed by
78 TcdB[33]. Bezlotoxumab, a monoclonal antibody against TcdB, has been adopted for clinical use in
79 conjunction with antibiotics for high-risk patients[23,34]. However, it poorly neutralizes the
80 prevalent TcdB2 variant, and clinically it is only partially effective in reducing recurrent CDI in
81 humans. Oral administration of polyclonal antibodies from cows hyperimmunized with TcdA
82 and TcdB has likewise been evaluated in human trials with reported success but has not
83 progressed to commercial development[35–37]. Most recently, fecal microbiota transplantation
84 (FMT) has also proven effective in reducing recurrence of CDI, presumably by helping to correct
85 the intestinal dysbiosis that predisposes to relapsing disease[38]. Despite these advances there
86 currently are no clinically approved therapeutics to prevent primary CDI. There are no FDA
87 approved CDI vaccines[39], and the most recent Phase 3 clinical trial of an anti-toxin vaccine was
88 terminated due to futility[40].

89 We report here the preclinical development of a four-component therapeutic cocktail to both
90 prevent and treat CDI. The cocktail is comprised of homodimeric versions of three toxin-binding
91 proteins (5D, E3, and 7F) derived from camelid single-domain antibody fragments known as
92 VHHs or nanobodies. Each protein was previously shown to inactivate TcdB[8,28,29,41]. Binding of
93 5D to TcdB prevents its pH-driven conformational change that enables pore formation and
94 transit into the cytoplasm from internalised endosomes. E3 binds to the glucosyltransferase
95 domain (GTD) of TcdB, interfering with the autoproteolysis step necessary for enzyme
96 activation. 7F also binds to the GTD, inhibiting catalytic glucosylation/inactivation of Rho-family
97 GTPases by the mature N-terminal glucosyltransferase. The fourth cocktail component is a
98 *C. difficile*-specific endolysin[42]. These proteins are highly specific, phage-encoded antimicrobial
99 lytic enzymes that, due their specificity and rapid effect, hold considerable promise for treating
100 bacterial infectious diseases, including CDI[42–44]. We showed that the selected combination of
101 three dimeric VHHs had a synergistic neutralization potency that vastly exceeded the potency
102 of any single dimeric VHH and had far greater potency and broader strain coverage than
103 bezlotoxumab[23,34]. We further demonstrated that the therapeutic was enhanced by combining
104 the dimeric VHHs that neutralize TcdB with an endolysin that destroys the *C difficile* bacterium.
105 LMN-201 was manufactured using the edible microorganism spirulina (*Arthrospira platensis*) as
106 the expression platform. It was delivered orally as a powder of whole, unrefined spirulina
107 biomass[45], and is easily scalable, shelf-stable, simple to administer, and broadly neutralizing
108 against all common TcdB types.

109

110 **RESULTS**

111

112 **Spirulina strain engineering**

113 The *C. difficile* therapeutic LMN-201 contained four therapeutic proteins: three homodimeric
114 fusion proteins designated pp1005, pp1006, and pp1007, which incorporated homodimeric
115 derivatives of VHHs 5D, E3 or 7F, respectively; and fourthly, the catalytic domain of the
116 bacteriophage-derived PlyCD endolysin, designated pp1092.

117 The primary structures of each monomer subunit in the VHH homodimers were similar. From
118 amino to carboxy terminus this was: the maltose-binding protein (MBP) chaperone (366 amino
119 acids)[46], a Gly-Gly-Gly-Gly tetrapeptide linker, a 5HVZ dimerization domain (49 amino acids), a
120 Gly-Ser-Gly-Ser-Gly-Gly peptide linker, a TcdB-binding VHH (111-127 amino acids), a Gly-Ser-Gly
121 tripeptide linker and a hexahistidine tag (543-562 amino acids total) (Figure 1A). The 5HVZ
122 dimerization domain was derived from the mammalian cAMP-dependent protein kinase A
123 (PKA) holoenzyme[47,48].

124 The endolysin PlyCD has been previously demonstrated to be *C. difficile* specific[42-44]. Full-length
125 PlyCD (pp1093) its catalytic domain alone, $PlyCD_{1-174}$ (pp1092), were expressed in spirulina
126 strains sp1286 and SP1287, respectively, with an N-terminal 6x his-tag (Figure 1A).

127 Genes encoding pp1005, pp1006, pp1007, pp1093 and pp1092 were engineered into the
128 spirulina chromosome by homologous recombination (Figure 1B)[45]. The final strains—SP1308,
129 SP1312, SP1313, SP1286 and SP1287, respectively—contained the gene of interest integrated
130 into the spirulina chromosome at a single, pre-selected location and no other exogenous

131 genetic information. Clonal spirulina filaments were then isolated by micromanipulation,
132 verified as being homozygous with respect to the transgene, and used to create a frozen strain
133 bank (Figure 1B, C)[45].

134 **Characterization of spirulina-expressed anti-TcdB VHHs: expression and binding kinetics**

135 Expression levels of all 5 candidate therapeutic proteins in spirulina were quantified using a
136 capillary electrophoresis-based immunoassay (Figure 2A). After growth in a bioreactor, dried
137 whole SP1308 biomass was comprised of 0.5% by weight pp1005; SP1312 was comprised of
138 2.3% pp1006; SP1313 was comprised of 3.4 % pp1007; and SP1287 was comprised of 0.5%
139 pp1092. At least 90% of each of these proteins was soluble following a one-hour extraction in
140 an aqueous buffer at neutral pH. The dimeric state of the VHHs on the 5HVZ scaffold was
141 confirmed by comparing their relative mobilities during size-exclusion chromatography, and by
142 capillary electrophoresis in reducing versus non-reducing conditions (Figure 2B). Intra-scaffold
143 disulfide bonds were present in the extracted proteins (Figure 2B) but were dispensable for
144 stable assembly of the 5HVZ-VHH dimers (Figure 2C).

145 Binding kinetics were measured by biolayer interferometry using recombinant subdomains of
146 TcdB that corresponded to the specific antigen-binding sites of each VHH homodimer
147 (Figure 3A, B). The apparent K_D's were in the mid- to low-picomolar range. The dimeric versions
148 of all three proteins displayed substantially greater apparent avidity for TcdB than the
149 corresponding monomeric versions (Figure 3B).

150 **Characterization of TcdB's effect on cell adhesion**

151 Disruption of the actin cytoskeleton by TcdB causes changes in cell shape and cell attachment.
152 *In vitro*, these cytoskeletal changes can be measured in real-time as a change in impedance
153 using cells cultured on a surface embedded with microelectrodes[49,50]. TcdB1 is the TcdB toxin
154 type most frequently present in worldwide *C. difficile* isolates from infected patients[51]. The
155 source of TcdB1 for these analyses was ribotype (RT) 087 (type strain 10463). The concentration
156 range of TcdB1 tested spanned the amounts reported in human patients with *C. difficile*
157 infection[52]. Data describing TcdB1 toxicity were collected and fit to a four-parameter sigmoid
158 using nonlinear regression to minimize the sums of residuals squared:

159 $$Adhesion = Top - (Top - Bottom) \cdot \frac{T^H}{T^H + {IC_{50}}^H}$$

160 where Adhesion indicates the results of the above cell attachment assay; Top and Bottom are
161 the highest (no TcdB1) and lowest (maximal TcdB1) assay values; T is the concentration of
162 TcdB1; IC_{50} is the concentration of TcdB1 eliciting half maximal inhibition in Adhesion; H is the
163 steepness of the concentration-response relationship.

164 The concentration of half-maximal inhibition of cell adhesion by TcdB1 was 1.268 fM with a Hill
165 slope coefficient of 1.495 (Table 1; Figure 4).

166 **Synergistic Inhibition of TcdB by anti-TcdB VHH homodimers**

167 Data were collected to evaluate inhibition of TcdB toxicity by each VHH homodimer, and all
168 two- and three-way combinations (Figure 4A; Supplemental Figure 1). Individually, each of the
169 dimeric VHHs had sub-nanomolar EC_{50} values for TcdB neutralization (Table 1). However,

170 compared to the single VHHs, the cocktail of the three dimeric VHHs showed remarkable
171 synergy, providing robust neutralization across the very wide range of TcdB concentrations
172 found in patients with CDI[52] (Figure 4; Supplemental Table 2). To illustrate, a concentration of
173 1.5 nM of any one of the three dimeric VHHs shifted the IC_{50} of TcdB1 10- to 60-fold, whereas a
174 1.5 nM cocktail of all three combined (0.5 nM each) shifted the IC_{50} of TcdB1 almost 3,000-fold.
175 For TcdB2 the cocktail synergy was similarly striking. At a concentration of 1.5 nM the individual
176 dimeric VHHs shifted the IC_{50} of TcdB2 10- to 150-fold, while a 1.5 nM cocktail of the three
177 dimeric VHHs (0.5 nM each) shifted the IC_{50} of TcdB2 more than 16,000-fold.

178 Surprisingly, the dramatic synergy of antibody combinations requires nothing more than that
179 they bind independently to distinct epitopes on the target. Quantitative modeling using
180 measured K_D's and the effects of dimeric VHH mixtures across a large range of TcdB
181 concentrations indicated that this was likely to be the entire explanation for the synergy we
182 observed (Supplemental Text and Supplemental Figures 1,2,3). This suggested that synergy
183 might be much more easily achieved than is generally appreciated, which has important
184 implications for the development of therapeutic antibody cocktails (see Discussion).

185 **Broad coverage of TdcB toxin-types**

186 Mansfield et al.[33] used *C. difficile* genomic sequences to define 12 distinct TcdB groups that
187 differed from each other by 3% or greater. 96% of the TcdB genes present in that dataset were
188 defined as belonging to groups 1, 2, 3, and 5. Group 1 is the most clinically prevalent group
189 worldwide, and group 2 is expressed by *C. difficile* ribotype 027, the single most prevalent strain
190 type in the United States, and second most prevalent in Europe[3,51,53,54].

191 The high degree of conservation of the pp1005, pp1006, and pp1007 binding sites[41] suggested
192 that each of the dimeric VHHs would neutralize most, if not all, of the four prevalent TcdB toxin
193 types, except for neutralization of TcdB group 5 by pp1005. We measured the IC_{50} values of
194 TcdB types 1.1, 2.1, 3.1, and 5.1 alone and when incubated in 1.5 nM pp1005, pp1006, pp1007,
195 or a cocktail comprised of all three VHH homodimers (0.5 nM of each) and compared these
196 with the neutralizing potency of 3 nM bezlotoxumab (Figure 4). Each VHH homodimer exhibited
197 strong neutralizing activity against all tested toxin types except pp1005, which was only weakly
198 active against toxin type 5. The triple VHH cocktail synergistically neutralized all tested toxin
199 types, with apparent relative potencies of against each toxin type of 2>1>3>5. Compared to the
200 triple VHH cocktail, bezlotoxumab was significantly less potent at neutralizing all tested toxin
201 types, and its neutralizing activity against toxin type 2 (ribotype 027) was notably weak.

202 **Characterization of spirulina-expressed anti-*C. difficile* lysin**

203 PlyCD, a prophage lysin, was found to have a high degree of specificity for degrading *C. difficile*
204 peptidoglycan[42]. The catalytic domain of this protein, $PlyCD_{1-174}$, efficiently lysed various strains
205 of *C. difficile* while leaving commensal bacteria unaffected, with rare exceptions that included
206 *B. subtilis* and *C. sordellii*.

207 Genes encoding pp1093 (full-length lysin PlyCD) and pp1092 ($PlyCD_{1-174}$) were engineered into
208 spirulina to produce strains SP1286 and SP1287, respectively. Expression of both proteins in
209 spirulina was quantified using a capillary electrophoresis-based immunoassay. After growth in a
210 bioreactor pp1093 comprised 0.1% of dry biomass and was approximately 50% soluble
211 following aqueous extraction. pp1092 comprised 0.5% of total SP1287 biomass, and after

212 aqueous extraction greater than 90% of pp1092 was soluble (Figure 5A). Following extraction
213 from SP1286 and SP1287 biomass the pp1093 and pp1092 proteins were found to be
214 monomeric by size-exclusion chromatography and non-reducing PAGE (Figure 5B). However,
215 pp1093 exhibited notable size heterogeneity, with lower molecular size species.

216 The lytic activities of pp1093 and pp1092 were compared in a turbidity reduction assay using
217 extracts from SP1286 and SP1287, and *B. subtilis* as the target bacterium. In these spirulina cell
218 extracts, the specific activity of pp1092 was 8-fold greater than pp1093 (Figure 5C). The
219 reduced lysin activity of the pp1093 compared to pp1092 was also observed using *C. difficile*
220 strain ATCC 43255 as the target bacterium (Supplemental Figure 4). The lytic activities of
221 pp1093 and pp1092 isolated from spirulina were not significantly different from the same
222 proteins isolated from *E. coli.* (Supplemental Figure 4). SP1287 (expressing pp1092) was
223 selected for inclusion in LMN-201 based upon its superior expression level, homogeneity and
224 bioactivity compared to SP1286. As a control for interference, it was shown that pp1092 did not
225 affect toxin neutralization by the anti-TcdB VHH cocktail (Figure 4).

226 **Stabilities of anti-TcdB VHHs and anti-*C. difficile* lysin**

227 The four therapeutic proteins within LMN-201 all demonstrated resistance to three common
228 intestinal proteases: trypsin, elastase, and chymotrypsin (Figures 6A, 7). When exposed to
229 conditions simulating constitutive levels of these proteases for one hour, pp1005, pp1006, and
230 pp1007 retained nearly 100% ELISA binding activity compared to undigested protein. At a
231 higher concentration of protease that simulated the induced protease amounts following a
232 meal, pp1005 and pp1006 exhibited some sensitivity to digestion with 0.1 mg/mL trypsin but

233 still retained 63% and 75% of their antigen-binding activities, respectively. SDS-PAGE and
234 western blotting demonstrated that chymotrypsin cleaved the MBP domain of these dimeric
235 toxin-binding proteins within 30 minutes, leaving the VHH-5HVZ dimer intact. This was
236 consistent with the observation that chymotrypsin did not reduce binding affinity as measured
237 by ELISA, and removal of the MBP moiety may explain the paradoxically increased ability to
238 detect bound VHH in an ELISA after chymotrypsin digestion. To confirm that digestion did not
239 affect bioactivity, chymotrypsin-digested pp1005, pp1006, and p1007 were also evaluated in a
240 cell-adhesion assay. No significant changes in toxin neutralizing activity were observed after
241 exposure to chymotrypsin for at least one hour (Figure 6B).

242 Protease treated pp1092 was analyzed for structural integrity by SDS-PAGE (Figure 7A), and for
243 bioactivity in a turbidity reduction assay using intact *B. subtilis* as the substrate (Figure 7B).
244 pp1092 showed no detectable change in molecular size (25kDa) following digestion with any of
245 the three proteases. In contrast, full length PlyCD (37kDa) was almost 100% cleaved to a smaller
246 25 kDa product by all three proteases, consistent with release of the smaller, protease-stable
247 catalytic subdomain. Further, pp1092 retained 100% bioactivity following digestion with any of
248 the three proteases at the lower level, and greater than 70% bioactivity following digestion with
249 higher (induced) protease amounts.

250 ***In vivo* efficacy**

251 Efficacies of cocktail therapeutics containing anti-TcdB VHH homodimers and anti-*C. difficile*
252 lysins were evaluated in mouse (Figure 8) and hamster (Figure 9) pathogen challenge models.

253 Cohorts of male C57BL/6J mice were infected with *C. difficile* spores 24 hours after
254 administration of one of the following treatments by oral gavage: vancomycin (positive
255 control); wild-type spirulina (negative control); Cocktail 1; or Cocktail 2. Cocktail 1 was
256 comprised of equal proportions of spirulina strains SP1308, SP1312, and SP1313 (expressing
257 pp1005, pp1006, and pp1007, respectively) and SP1286 (expressing pp1093). Cocktail 2 was the
258 same but omitted SP1286. Each treatment was then administered once daily following
259 *C. difficile* challenge.

260 The largest number of *C. difficile* spores was shed by mice treated with wild-type spirulina
261 (Figure 8A). Treatment with Cocktail 1 significantly reduced fecal spore shedding at 24 hours
262 post infection and at the time of euthanasia ($10^{2.206}$ and $10^{1.867}$ cfu/g lower, respectively), than
263 wild-type spirulina controls and significant by t-test with $p=0.0175$ and $p<0.001$ (Supplemental
264 Table 3). Fewer spores were observed shed by animals treated with only the toxin-neutralizing
265 antibodies (Cocktail 2), but the difference did not reach statistical significance at either
266 timepoint.

267 The largest maximum weight loss was observed in the negative control group, mice treated
268 with wild-type spirulina, 3.922 g (Figure 8B; Supplemental Table 4). Treatment with either
269 spirulina cocktail or vancomycin all reduced the maximum weight loss significantly. On average,
270 the maximum weight lost by an individual treated with Cocktail 1 was 2.057 g less than the
271 group treated with wild-type spirulina and significant by t-test with $p<0.01$. The maximum
272 weight lost by subjects treated with Cocktail 2 was 2.102 g, a result significant by t-test with
273 $p<0.001$.

274 Treatment with the spirulina therapeutic Cocktails 1 and 2 also increased survival rates, with
275 borderline significance possibly due to small sample size (Figure 8C). None of the mice treated
276 with Cocktail 1 perished due to *C. difficile*-related causes (4/4, 100% survival) which was
277 equivalent to the vancomycin-treated group (10/10, 100% survival). The increased survival rate
278 was borderline significant relative to the wild-type spirulina-treated group by log-rank test with
279 p=0.079. The group treated with Cocktail 2 also exhibited higher survival rates than the
280 negative control (6/7, 87% compared to 2/5, 40%) with borderline significance by log-rank test
281 with p=0.14. The mouse efficacy study suggests that a spirulina anti-TcdB cocktail
282 supplemented with the lysin is effective at reducing bacterial load and improving clinical
283 outcomes *in vivo*.

284 The Golden Syrian Hamster model of CDI has been used previously for evaluating orally
285 delivered antibodies against *C. difficile* toxins[30]. The experimental groups we used were
286 Cohort 1: no treatment, Cohort 2: wild-type spirulina, Cohort 3: anti-TcdB VHHs (3) + Anti-TcdA
287 VHHs (2) + lysin PlyCD, all delivered within whole spray-dried spirulina biomass. Each treatment
288 was administered twice daily by oral gavage, from days -1 through day 12. It was necessary to
289 include anti-TcdA VHHs in this protocol because TcdA contributes significantly to disease in
290 hamsters (unlike in humans)[8]. We observed that the therapeutic protein cocktail significantly
291 extended survival time compared to the wild-type spirulina control (p=0.015) (Figure 9A), and
292 significantly reduced *C. difficile* colonization of the cecum by more than an order of magnitude
293 when compared to untreated or wild-type treated groups (p=0.046 and p=0.0041, respectively)
294 (Figure 9B).

295 **DISCUSSION**

296 We report here the first use of quantitative analyses of drug synergy for preclinical and clinical
297 development of a therapeutic antibody cocktail. These analyses build on a general framework
298 for evaluating the effects of multiple drugs acting on a single target that was initially developed
299 to model enzyme inhibition[55]. In that context it was shown that mutually exclusive inhibitors
300 (i.e., competitive) have an additive inhibitory effect, whereas mutually nonexclusive inhibitors
301 (i.e., independent) have a multiplicative (i.e., synergistic) effect. This framework can be applied
302 more generally, for example to antibody inhibitors of a protein[56], and has the potential to
303 inform decisions around drug cocktail formulation, including selection of lead candidates and
304 optimization of their relative concentrations.

305 Synergy is usually not considered in the development of cocktail therapeutics. To some degree
306 this is due to the costs and complexities associated with developing drug combinations, but it is
307 also because such synergies are often thought to be rare, arising from cooperative or unusual
308 allosteric effects[57]. A small number of anti-viral therapeutics have been intentionally developed
309 as antibody cocktails[58,59], but this was done to reduce the likelihood of pathogen escape.
310 Moreover, if drug concentrations are only evaluated within a 2- or 3-fold range of their
311 respective EC_{50} values, synergy can be difficult to distinguish from simple additivity, and is
312 therefore easily overlooked. Accordingly, almost all clinically approved antibody cocktails were
313 first developed as solo therapeutics, and subsequently only a small subset have been
314 empirically evaluated in combination, often without regard to understanding whether
315 underlying synergies might have contributed to improved efficacy.

316 In contrast to the prevailing view that synergy is rare and elusive we have demonstrated here,
317 using the specific example of anti-*C. difficile* toxin antibodies, that synergy can simply be the
318 result of the laws of mass action governing the independent interactions of drugs with a
319 common target, and therefore may be more readily achieved than is generally thought.
320 Moreover, the synergistic efficacy of independently acting drugs increases nonlinearly with
321 concentration and can be enormous when concentrations substantially exceed the EC_{50}. We
322 emphasize that this is not a complex function of allostery or cooperativity, but a simple
323 consequence of independent Michaelis-Menten binding. This has general and important
324 implications for therapeutic development. Synergistically acting antibodies will be particularly
325 useful for treating a disease like CDI, where single antibody therapeutics struggle to achieve the
326 very high level of target inhibition required. That the cocktail also offers broader strain
327 coverage and protection against escape variants adds to its appeal.

328 Beyond infectious diseases, antibody synergy may also be important for treating diseases with
329 complex etiologies where single-agent interventions have only been moderately successful, for
330 example inflammatory diseases of the gastrointestinal tract and cardiometabolic disease. The
331 results here offer antibody drug developers a paradigm for developing high potency cocktail-
332 based interventions against diseases refractory to single-antibody approaches.

333 CDI is an appealing initial target for clinically evaluating these principles, because current
334 therapies for preventing recurrent CDI are only partially successful, and there are no options
335 available to prevent initial bouts of CDI in at-risk populations. LMN-201 is a spirulina-expressed
336 and orally delivered cocktail of four therapeutic proteins that target both the *C. difficile*

337 bacterium and the key driver of its virulence, exotoxin TcdB. Orally delivered protein
338 therapeutics may offer significant advantages over their injected counterparts for treatment
339 and prevention of recurrent CDI. Oral administration can deliver high amounts of therapeutic
340 proteins directly to the intestine epithelium, whereas systemically delivered antibodies have
341 poor partitioning coefficients from the vasculature to the gut lumen[60]. Moreover, the risk of off-
342 target toxicity is reduced: the therapeutic proteins within LMN-201 are too large for intact
343 systemic absorption[45]. At least three prior clinical trials have reported safe and efficacious oral
344 administration of bovine antibodies against *C. difficile* toxins derived from milk or colostrum[35–
345 37], supporting the feasibility of this approach.

346 The harsh environment of the gastrointestinal tract is considered challenging for orally
347 delivered protein therapeutics. LMN-201 addresses this challenge in several ways. First, the
348 therapeutic proteins in LMN-201 showed significant resistance to the major GI proteases.
349 Second, for human administration the product is delivered orally in polymer-coated capsules
350 designed to release the drug product in the ileum. Third, spirulina-based cGMP manufacturing
351 is highly scalable, making feasible cost-effective administration of the drug product throughout
352 the period of high risk for CDI recurrence, even if the harsh GI environment necessitates daily or
353 twice daily administration to maintain therapeutic levels at the site of action[42].

354 Perhaps of greatest significance is the extraordinary potency of LMN-201: each dimeric VHH
355 within LMN-201 had a sub-nanomolar EC_{50} for TcdB inhibition, and this was substantially
356 enhanced by cocktail formulation. An oral dose of 1,500 mg of spirulina biomass (500 mg of
357 each VHH-spirulina strain) will deliver to the intestine a combined dimeric VHH concentration of

358 approximately 2.6 µM, which is more than 1,000-fold higher than minimally required[61,62].
359 Pharmacokinetic data from a Phase 1 trial of LMN-201 confirmed that the amount of bioactive
360 VHH recovered in the distal ileum following oral administration was more than sufficient to
361 neutralize TcdB-levels previously reported in patients at risk for CDI recurrence (manuscript in
362 preparation).

363 The fourth LMN-201 component—a bacteriophage-derived endolysin—not only broadens
364 *C. difficile* strain coverage but also enhances efficacy. While TcdB is the key virulence factor in
365 CDI, approximately 5% of patients are infected by *C. difficile* strains that secrete TcdA but not
366 TcdB[52]. Other virulence factors are also associated with CDI, including the *C. difficile* binary
367 toxin (CDT), which is associated with increased 30-day mortality[63]. Inclusion of the lysin may
368 offer protection against these non-canonical *C. difficile* strains, as well as novel strains with new
369 toxin variants that might emerge in the future.

370 The lysin may also increase therapeutic potency in at least two ways. First, clinical performance
371 is augmented by the lysin's previously demonstrated synergy with standard-of-care
372 vancomycin, which act in concert to disrupt *C. difficile* cell wall structure[42]. Second, these
373 agents independently intervene at two steps in the pathway that controls virulence—*C. difficile*
374 proliferation and toxin action on the gastrointestinal epithelium. The lysin thus complements
375 the VHH homodimers with a potential for orthogonal synergy to enhance LMN-201's clinical
376 real-world effectiveness.

377 **MATERIALS AND METHODS**

378

379 **Engineering of spirulina**

380 Markerless spirulina strains were generated as described[45]. In brief, the natural spirulina gene
381 WP_006618409.1, which confers resistance to kanamycin, was replaced with an exogenous
382 gene encoding resistance to streptomycin to generate spirulina strain SP205. SP205 was then
383 transformed with constructs containing the gene of interest, WP_006618409.1, as well as the
384 homology arms. The transformants were selected with kanamycin. Single filaments were
385 isolated and propagated to generate cell banks. Cells were then thawed from the cell banks and
386 DNA was extracted to be used to confirm complete segregation and verify sequence of the
387 WP_006618409.1 via PCR and Sanger Sequencing.

388 **Illumina sequencing of spirulina**

389 Spirulina genomic DNA was extracted using a Blood and Tissue Kit (Qiagen, 69504) with minor
390 modifications. Spirulina biomass was resuspended in buffer ATL. It was digested with
391 proteinase K (2 mg/mL) overnight at 56 °C and then treated with RNase A (10 mg/mL) for
392 20 minutes at 56 °C. 400 µL of buffer AL was added and the biomass was pelleted for 10
393 minutes at 13,000g. The supernatant was then transferred to a fresh tube with 250 µL of 100%
394 ethanol, mixed and applied to DNeasy columns. The samples were washed once with 500 µL
395 buffer AW1 and once with 500 µL AW2 and eluted using molecular grade water. The amount of
396 genomic DNA was quantified by a Qubit dsDNA HS Kit (Thermo, Q33230) and prepared for
397 Illumina analysis using the Illumina DNA prep kit (Illumina, 20018704). Illumina sequencing of

398 the spirulina genome was performed on a MiSeq instrument using a MiSeq Reagent Kit v2
399 (Illumina, MS-102-2003).

400 **Illumina dataset analysis for copy number determination**

401 Copy numbers of the genes of interest in SP1287, SP1308, SP1312, and SP1313 were
402 determined by comparing expression of the transgenes to 10 randomly selected genes
403 (referred to as "normalization genes": *ppaX, rpsA, chlM, degU2, radA, rbcL, sdhA, psbC, cysA1,*
404 *smc6*) in the genome. A copy number of about 1, within plus/minus 0.15, was expected and set
405 as the benchmark for a full genomic integration of 1 gene per genome copy. As a validation
406 control, we also chose a second set of 10 random spirulina genes (*thrB1, hisC1, isfD2, pilA, purB,*
407 *apcE, nblA, gpmB, bicA2, cpcBA*) which we compared pairwise to the "normalization genes" set
408 in a manner identical to the transgene. Gene copy number per genome was determined by first
409 using samtools (http://www.htslib.org/doc/) to generate an mpileup file with Illumina reads per
410 base pair. Then, the median read per base pair was determined across the 10 "normalization
411 genes" and the transgene. The median read per base pair of the transgene was then divided by
412 the 10 "normalization genes" median read-per-base-pair value.

413 **Preparation of spirulina extracts for analysis of soluble protein**

414 Soluble extracts from spray-dried or paste samples were prepared by bead beating in a
415 Percellys evolution bead beater (Bertin Technologies). Beads for this procedure were purchased
416 in pre-packed tubes from MP-Bio (cat# 6911500). Dried spirulina biomass was resuspended in
417 PBS containing Pierce Protease Inhibitor minitablets and 1 mM PMSF at a biomass
418 concentration of 2-10 mg/mL. Biomass samples were then centrifuged at 15,000g at 4 °C for 30

419 minutes, and the soluble fraction was transferred to a separate tube for downstream
420 applications.

421 **Expression analysis of soluble recombinant proteins in spirulina**

422 Recombinant protein expression in spirulina was measured by capillary electrophoresis
423 immunoassay (CEIA) using a Jess system (ProteinSimple). The Jess system was run as
424 recommended by the manufacturer. Briefly, dried biomass samples were diluted to a
425 concentration of 0.1-1 mg/mL using water and a 5X master mix prepared from an EZ Standard
426 Pack 1 (Bio-Techne). Purified protein controls used to generate standard curves were typically
427 loaded at a range of concentrations from 0.25-8 µg/mL. A 12-230 kDa Jess/Wes Separation
428 Module (ProteinSimple) was used for separation. A mouse anti-His-Tag antibody (GenScript)
429 was diluted 1:100 and used as the primary antibody. An anti-mouse NIR fluorescence-
430 conjugated secondary antibody (ProteinSimple) was primarily used for detection. Non-reducing
431 denaturing gels were performed in the same manner; however, reductant was withheld from
432 the 5X master mix. Data analysis was performed using the Protein Simple Compass software
433 and Microsoft Excel.

434 **Expression analysis of total recombinant proteins (soluble and insoluble) in spirulina**

435 Spray dried or paste samples were prepared by bead beating as above. The samples were
436 solubilized in PBS buffer mentioned above with a Triton X-100 concentration at 0.02%.
437 Following lysis, samples were diluted to 0.1-1 mg/mL in extraction buffer (60 mM dithiothreitol,
438 60 mM Na_2CO_3, 6 mM ethylenediamine tetraacetic acid, 2% (w/v) sodium dodecyl sulfate,
439 12% (w/v) sucrose and 0.02% Triton X-100). After the addition of the lysis buffer, samples were

440 immediately heated at 100 °C for 120 seconds, then centrifuged at 16,000g for 5 minutes.
441 Extracted samples were displayed on the Jess system as described above.

442 **Cell lines, bacterial strains, toxins, and antibodies**

443 Vero cells (ATCC) were cultured in Dulbecco's Modified Eagle Medium (DMEM) supplemented
444 with 10% heat-inactivated fetal bovine serum and 1% penicillin-streptomycin (Gibco). The cells
445 were grown in a high-humidity incubator at 37 °C and 5% CO_2. *C. difficile* toxin TcdB-10463 was
446 expressed in *B. megaterium* (a gift from C. Shoemaker, Tufts University) and purified using Ni-
447 NTA affinity and ion exchange chromatography. Purified *C. difficile* toxins TcdB-027, TcdB-1470,
448 and TcdB-078 were purchased from tgcBIOMICS. Bezlotoxumab was sourced from Henry Schein
449 Medical.

450 **Expression of TcdB fragments in bacterial systems**

451 The VHH-binding domains on TcdB[41] were designed for bacterial expression with an N-terminal
452 hexahistidine tag followed by MBP and TEV protease recognition site (ENLYFQG) and C-terminal
453 Avi-tag (LNDIFEAQKIEWHE) for enzymatic biotinylation. Based on the structural information, we
454 designed the 5D-binding region, the delivery and receptor-binding domain (DRBD) of TcdB for
455 expression using residues from amino acid position 1092 to position 1433 of TcdB. VHHs 7F and
456 E3 bind regions on the glucosyltransferase domain (GTD). A fragment containing this region was
457 designed to include amino acid positions 2 through amino acid 543 of TcdB. The constructs
458 were subcloned into a modified pET28 b(+) vector where the Kanamycin bacterial resistance
459 gene was replaced with Ampicillin bacterial resistance gene. Constructs were sequence verified
460 by Sanger sequencing (Genewiz). Sequence verified plasmids were transformed into BL21(DE3)

461 *Escherichia coli* cells (New England Biolabs) and plated on LB medium supplemented with 100
462 μg mL^{-1} ampicillin. Protein was expressed using autoinduction protocol[64]. Briefly, 1 L of Super
463 Broth media containing appropriate selection drug was inoculated with overnight cultures from
464 individual transformants, shaken at 37 °C for 8 hours followed by 16 °C for 24 hours. Expression
465 cultures were pelleted by centrifugation and stored at −20 °C until purification. Frozen cell
466 pellets were thawed on ice and resuspended in 100 mL of 50 mM Tris pH 8.0, 300 mM NaCl
467 supplemented with pierce protease inhibitor tablets EDTA free (Thermo Fisher Scientific cat. no.
468 A32965) and 1 mM phenylmethylsulfonyl fluoride (PMSF) (Thermo Fisher Scientific cat. no.
469 36978). Cells were lysed by high pressure homogenization (HPH) (Microfluidics LM20) at 12,000
470 psi. The lysates were clarified by centrifugation at 18,500*g* at 4 °C for 30 minutes using tabletop
471 centrifuge (Eppendorf Centrifuge 5810R). Soluble protein was separated from cell debris and
472 the supernatant was passed through 5 mL HisTrap columns (Cytiva, cat. no. 17524802)
473 equilibrated with 50mM Tris pH 8.0, 300 mM NaCl and 20 mM imidazole (Thermo Fisher
474 Scientific, cat. no. O3196-500). His-tagged protein bound HisTrap columns were washed with 10
475 column volumes (CV) wash buffer (50 mM Tris, pH 8.0, 300 mM NaCl and 20 mM imidazole).
476 Bound his-tagged protein were eluted using gradient flow at slope of 10% - 100% elution buffer
477 (50 mM Tris pH 8.0, 300 mM NaCl and 250 mM imidazole) in 5 CV. Fractions containing the
478 eluted protein were assessed by SDS-PAGE gel. SDS-PAGE analyses were performed by
479 incubating 2 μL of purified protein elution in NuPAGE LDS Sample Buffer (Thermo Fisher
480 Scientific) at 70˚C for 10 minutes. Bis-Tris NuPAGE 4 to 12% gels were placed into gel box filled
481 with NuPAGE MES SDS Buffer. Samples were loaded and gels run at constant volt of 170 mV for
482 40 minutes, followed by staining using Coomassie Blue gel stain. Fractions were pooled based

483 on level of purity, concentrated, and buffer exchanged into PBS. The samples were then filtered
484 through a 0.2 μm filter and run over a size-exclusion column on AKTA Pure FPLC-based size-
485 exclusion chromatography HiLoad 16/600 Superdex 200 pg column (Cytiva, cat. no. 28989335)
486 equilibrated in PBS. Purity and final analysis were performed using SDS-PAGE gel where 3 μg
487 purified protein samples were incubated at 70 °C in LDS loading buffer with or without 20 mM
488 dithiothreitol (DTT) reducing agent (Thermo Fisher Scientific, cat. no. R0862). Protein samples
489 were separated by size on NuPAGE Bis-Tris gels as described above. Purified samples were
490 biotinylated using BirA biotin ligase (Avidity Inc.) at 1 μg of BirA enzyme per 10 nM of protein.

491 **Protein purification from spirulina biomass**

492 The TcdB-binding proteins developed from VHHs 5D (pp1005, batch no. 145), E3 (pp1006, batch
493 no. 147), and 7F (pp1007, batch no. 147), and full-length lysin PlyCD (pp1092, batch no. 025)
494 were expressed in spirulina and purified from spray-dried biomass using Ni-NTA affinity and
495 size-exclusion chromatography 2-step purification protocol. Dried spirulina biomass from
496 strains expressing heterologous proteins were rehydrated at 30 mL/g of biomass in phosphate
497 buffer saline lysis buffer supplemented with protease inhibitor mix of 1 mM
498 phenylmethylsulfonyl fluoride (PMSF), (Thermo Fisher Scientific cat. no. 36978) and Pierce
499 Protease Inhibitor Tablets, EDTA-free, (Thermo Fisher Scientific cat no A32965). Rehydrated and
500 homogenous biomass resuspension were lysed using a high-pressure homogenizer
501 (Microfluidics LM20) at 12,000 psi. The lysates were clarified by centrifugation at 18500*g* on
502 tabletop Centrifuge (Eppendorf Centrifuge 5810R) for 30 minutes. Supernatant were clarified
503 by filtration using a coffee filter followed by 0.22 μm membrane filter. Recombinant proteins
504 were purified from the clarified lysate by affinity chromatography as describe above using 5 mL

505 HisTrap columns (Cytiva, cat. no. 17524802). Hexa-Histidine tagged and HisTrap-purified
506 samples were further refined using AKTA Pure FPLC-based size-exclusion chromatography on
507 HiLoad 16/600 Superdex 200 pg column (Cytiva, cat. no. 28989335). Protein purity and sizing
508 were assayed by size-exclusion chromatography on analytical Superdex 200 increase 10/300
509 (Cytiva, cat. no. 28990944) where 100 µL of purified protein at ~1 mg/mL was run in PBS.
510 Purified protein samples were also assessed on SDS-PAGE under reducing and non-reducing
511 conditions. 3 µg protein samples were incubated at 70 °C in LDS loading buffer with or without
512 20 mM dithiothreitol (DTT) reducing agent (Thermo Fisher Scientific, cat. no. R0862). Proteins
513 were determined to be >90% pure and exhibited the expected molecular weight size
514 distribution.

515 **Native gel analysis**

516 To assess the importance of disulfide bonds in pp1005, pp1006, and pp1007 dimer formation,
517 we compared protein migration in native and SDS-PAGE gel under reduced and non-reduced
518 conditions. Native gel analysis was performed following the manufacturer's recommendation
519 (Life Technologies) where 1 µg of purified protein was mixed with Native Page Sample Buffer
520 supplemented with or without 20 mM DTT. Native page anode buffer was prepared by mixing
521 50 mL NativePage 20X running buffer and 950 mL single distilled water. Similarly, 1 x
522 NativePage Dark Blue Cathode buffer was prepared by mixing 50 mL NativePage 20 x Running
523 buffer with 50 mL NativePage 20X Cathode Additive and 900 mL single distilled water. Gel
524 boxes were set up on ice and samples were loaded prior to adding running buffer. Inner
525 chamber of gel box was filled with NativePage Dark Blue Cathode buffer while the outer

526 chamber was filled with NativePage Anode buffer. Gels were run at a constant 150 V for 2.5
527 hours. Comparable sample preparations were run in SDS-PAGE gel as described above.

528 **Assessment of VHH binding to TcdB fragments with bio-layer interferometry (BLI)**

529 BLI measurements were performed on the Octet RED96 system (ForteBio) using High Precision
530 Streptavidin (SAX) Biosensors (ForteBio). Biosensors were hydrated with phosphate buffer,
531 pH 7.4 at room temperature for 10 minutes on Microplate 96-well flat-bottom (Greiner,
532 655209). All kinetics experiments were performed at 30 °C temperature with 500 rpm agitation
533 in the kinetics module. Biosensors were dipped into PBS containing wells for 60 seconds prior to
534 antigen loading. Biosensors were loaded with enzymatically biotinylated TcdB antigen
535 fragments at 10 µg/mL in phosphate buffer, pH 7.4 for 200 seconds to achieve ~0.6 – 1 nm
536 response. Loading was quenched by incubating biosensors in 50 µM Biocytin (Sigma Aldrich,
537 576-19-2) for 60 seconds. Baseline were established by incubating antigen loaded biosensors in
538 kinetics buffer (PBS + 0.02 % Tween 20, 0.1 % BSA, 0.05 % sodium azide) for 300 seconds. After
539 stablishing baseline, the rate of association was measured by incubating antigen loaded
540 biosensor tips into 3-fold dilution series of monomeric (pp1239, pp1238, and pp1240
541 respectively) or dimeric (pp1005, pp1006, and pp1007 respectively) 5D, E3, and 7F constructs.
542 The concentration series used to determine binding kinetics of pp1238 were 93.6 nM, 31.2 nM,
543 10.4 nM, 3.47 nM, 1.16 nM, and 0.36 nM. Concentrations used to determine binding kinetics of
544 pp1239 were 93.6 nM, 31.2 nM, 10.4 nM, 3.47 nM, 0.38 nM, and 0.38 nM. Concentrations used
545 for pp1240 were 92.2 nM, 30.7 nM, 10.2 nM, 3.41 nM, 1.14 nM and 0.38 nM. pp1005 was
546 assayed at 16.2 nM, 5.39 nM, 1.8 nM, 0.60 nM, 0.20 nM and 0.07 nM. Concentrations used for
547 pp1006 were 16.8 nM, 5.6 nM, 1.87 nM, 0.62 nM, 0.21 nM, and 0.07 nM. pp1007 were assayed

548 at concentrations of 84.9 nM, 28.3 nM, 9.43 nM, 3.14 nM, 1.05 nM, and 0.35 nM. Analyte
549 bound biosensors were dipped into kinetics buffer for 300 - 600 seconds to measure rate of
550 dissociation. Kinetic analysis was performed using the HT 11.1.1.39 Data Analysis module
551 (ForteBio). Results were double referenced. Both association and dissociation steps were used
552 in 1:1 binding model global data fitting model.

553 **Toxin-neutralization assay**

554 Toxin-neutralization assays using TcdB1.1, TcdB2.1, TcdB3.1 and TcdB5.1 were performed using
555 the Agilent xCELLigence RTCA MP. This system measures cell adherence via biosensors in the
556 bottom of a 96-well plate by applying a small electric current across microelectrodes. A unitless
557 measurement called cell index (CI) was then calculated based on changes in electrode
558 impedance. Because adherent cells increase electrode impedance, toxin induced cell rounding
559 can be determined from changes in CI.

560 Agilent 96-well E-plates were seeded with 100 µl/well of 1 x 10^5 cells/mL in DMEM culture
561 medium with 10% FBS and 1% Pen/Strep and allowed to rest for 30 minutes before going into
562 an xCELLigence real-time cell analyzer in a Caron CO_2 37 °C incubator to run overnight. CI was
563 monitored every 15 minutes for 20 to 24 hours. TcdB was serially diluted in culture medium in a
564 96-well set up plate. The VHH homodimer, lysin, and bezlotoxumab samples were diluted in
565 medium and then added to the serially diluted toxin. The TcdB/protein mixture was incubated
566 at 37 °C for 1 hour. After 1 hour, media was carefully removed from the cells seeded onto the E-
567 plates and 100 µL of the VHH homodimer and toxin mixture was added to the cells in each well.
568 CI was monitored every 15 minutes for at least 24 hours. Each run included a TcdB only

569 standard curve as a positive control and cells only as a negative control. VHH homodimer was
570 also tested in the absence of TcdB to assess any effects of VHH alone on CI. At the 24-hour time
571 point after treatment, the CI measurements for each well were normalized by setting the CI to
572 1 at the last reading taken before treatment was added. The normalized cell index (nCI) was
573 plotted using Prism and a nonlinear regression analysis was performed to calculate the IC_{50} of
574 TcdB under treatments.

575 **TcdB's effect on cell adhesion and inhibition of TcdB by anti-TcdB VHH homodimers**

576 Cell adhesion assay data were imported, normalized, and analyzed using R (version 4.1.1 The R
577 Foundation for Statistical Computing). Nonlinear regression was performed using the
578 *minpack.lm* routine in the *nlsLM* package, which implements the Levenberg-Marquardt
579 algorithm to perform bounded minimization[65].

580 **Lysin activity assay**

581 The lytic activity of pp1092 against *Bacillus subtilis* SL4 was assessed based upon previously
582 described methods with modifications to adapt the assay to a 96-well plate format[42]. Mid-log
583 phase grown SL4 were grown in BHI (37 °C, 250 rpm) harvested and washed twice in PBS by
584 centrifugation (room temperature, 6,000g, 10 minutes). Bacteria were then combined with 1ug
585 digested or undigested pp1092 in a final volume of 200 µL (OD = 1.0) and then turbidity
586 reduction was measured over time (37 °C, shaking). Each unknown was fit along with 5 3-fold
587 serial dilutions of undigested standards using a modified 5-parameter nonlinear logistic model.
588 The time of 50% OD_{600}, TC_{50}, was estimated as a 4-parameter nonlinear logistic model with lysin
589 concentration as the independent variable. For the standards, this concentration is known. For

590 the unknown sample, this value is estimated. All results were expressed as the mean ± standard
591 deviation as calculated by Excel software (v16.48, Renton, WA). Standard curves were
592 determined by linear regression analysis by Excel software (v16.48, Renton, WA). EC_{50} values
593 were calculated using GraphPad Prism (version number, GraphPad Software Inc, San Diego, CA).

594 For comparison of spirulina-expressed and *E. coli*-expressed PlyCD, *C. difficile* strain ATCC 43255
595 was grown to mid-log phase (optical density at 600 nm (OD_{600nm}) = 0.5) at 37 °C under
596 anaerobic conditions in reduced Brain Heart Infusion Medium (BD Biosciences) supplemented
597 with 0.5% (wt/vol) yeast extract and 0.1% (wt/vol) L-cysteine. The bacteria were harvested at
598 4,000 rpm for 15 minutes, washed and resuspended to an OD_{600nm} of 2.0 in 50 mM sodium
599 phosphate, pH 7.0. Using a 96-well nontreated polystyrene microtiter plate (Corning), 100 μL of
600 buffer with or without (untreated controls) lysin at initial concentrations ranging from 4 to 256
601 μg/mL were added to individual wells. Following the addition of 100 μL bacteria, the OD_{600nm} of
602 each sample was measured every 60 seconds for a total of 15 minutes at 37°C using a
603 SpectraMax M5 microplate reader (Molecular Devices). All data represents the average of
604 triplicate experiments.

605 **VHH homodimer protease digestion for ELISA and neutralization assays**

606 *In vitro* protease digestions of anti-*C. difficile* VHH homodimers were prepared in a matrix of
607 soluble lysate from wild-type spirulina (SP003) in Bis-Tris buffer pH 6.0 and treated with trypsin,
608 chymotrypsin, or elastase. VHH homodimers in PBS at were diluted in SP3 lysate, Bis-Tris buffer,
609 and protease so that the final concentrations were VHH homodimer, 20 mg/mL of SP3 lysate,
610 and a “fed” or “fasted” amount of protease. This level of SP3 lysate and VHH homodimer

611 simulates a expression level of 1% in spirulina (by dry weight). For trypsin and chymotrypsin,
612 the “fed” and “fasted” levels of protease in the digestion reactions were 0.1 and 0.01 mg/mL,
613 while for elastase, 5 and 0.5 µg/mL were used respectively. Samples were incubated at 37 °C for
614 1 hour with shaking at 900 rpm in an Eppendorf ThermoMixer. At the end of the incubation,
615 reactions were quenched with an equal volume of stop buffer containing 2 mM PMSF and 2x
616 Pierce protease inhibitor minitablet (Thermo Fisher) in PBS; elastase digests were additionally
617 neutralized with a 1 mM elastase inhibitor III. Samples were kept on ice until preparation for
618 ELISA or cell rounding assay. The final concentration of each VHH homodimer after protease
619 neutralization was 0.1 mg/mL.

620 **VHH homodimer quantitation by ELISA**

621 Digested VHH homodimers were analyzed for binding activity via ELISA using TcdB. Thermo
622 Scientific Nunc ELISA plates were coated with 100 µL/well of inactive TcdB at 2 µg/mL in CBC
623 binding buffer and incubated overnight at 4 °C. Plates were washed 3 times with PBS
624 supplemented with 0.05% Tween-20 (PBS-tw), then blocked for 1 hour with 300 µL/well of
625 block (PB-tw supplemented with 5% BLOTTO). Dilutions of undigested and digested VHH
626 homodimer were prepared in a low-binding 96-well plate by serially diluting with block. 6
627 dilutions of each undigested VHH homodimer were prepared for a standard curve. Two
628 dilutions of each protease digested sample were prepared for quantification by interpolation
629 from the standard curve. A 100 µL sample of each VHH homodimer was added to ELISA plate
630 wells and incubated for 1 hour at room temperature on a plate shaker. The plates were washed
631 as before. An HRP-conjugated anti-camelid VHH antibody cocktail (Genscript) was diluted
632 50,000-fold in block and 100 µL/well was added to the ELISA plates for 50 minutes with shaking.

633 Plates were washed 2 times with PBS-tw and 1 time with PBS. Finally, 100 µL/well of TMB Ultra
634 ELISA substrate (Thermo Fisher) was added to each well. The plates were developed in the dark
635 at room temperature on a plate shaker for 10 minutes before being quenched with 50 µL of 2.5
636 M sulfuric acid, and the absorbance was read at 450 nm with a Spectra Max M5 plate reader.
637 All digestion reactions were in duplicate, in 3 independent experiments.

638 **Calculation of VHH homodimer protease resistance**

639 The concentration of VHH homodimer in the protease-digested samples was calculated by
640 interpolating the concentration from standard curves generated with undigested VHH
641 homodimer. The percentage of remaining VHH homodimer activity after digestion was
642 calculated by dividing the interpolated value by the amount present if no VHH homodimer were
643 digested. Each replicate was calculated separately, and the average and standard deviation
644 were determined across all replicates.

645 **Toxin neutralization assay of digested VHH homodimer s**

646 Chymotrypsin-digested pp1005, pp1006, and pp1007 were assessed for toxin-neutralizing
647 activity as described. The final concentration of pp1005, pp1006, and pp1007 was 0.05 nM,
648 5 nM, and 5 nM respectively and the TcdB was 1:5 serially diluted starting at 250 pM.

649 **Lysin digestion conditions**

650 In digestion buffer (20 mM Tris, 150 mM NaCl, 3 mM $CaCl_2$ at pH 6.4) 0.2 µg/µL protein was
651 mixed with proteases trypsin (Promega sequencing grade), chymotrypsin (BD), and elastase
652 (BD) at 0.1 µg/µL or 0.01 µg/µL and incubated for 1 hour at 37 °C (200 rpm shaking). Reactions
653 were immediately quenched by addition of 1 mM PMSF and Protease Inhibitor Mini Tablets,

654 EDTA-free (Thermo Scientific, Pierce). For samples with elastase, 1 mM elastase inhibitor III
655 (Milipore Sigma) was added as well. To visualize digestion, 2 µg of digested and undigested
656 proteins were displayed a gradient BOLT-PAGE gel at 200 V for 20 minutes and then stained
657 with Coomassie.

658 **Densitometry**

659 Pixel intensity of Coomassie stained proteins were measured using ImageJ software,
660 normalizing all bands to the undigested band for each condition after subtracting background
661 pixel intensity of an identically sized bounding box.

662 **Preparation of *C. difficile* spores for mouse study**

663 *C. difficile* strain M7404, a ribotype 027 clinical isolate from Canada, was cultured on HIS-T agar
664 (3.7 % (w/v) heart infusion (HI) (Oxoid), 0.5 % (w/v) yeast extract, 1.5 % (w/v) agar
665 supplemented with 0.375 % (w/v) glucose, 0.1 % (w/v) L-cysteine and 0.1 % (w/v) sodium
666 taurocholate (New Zealand Pharmaceuticals)) in an anaerobic chamber (Don Whitley Scientific)
667 with an atmosphere of 10 % H2, 10 % CO_2 and 80 % N2 at 37 °C. To prepare spores, strains were
668 sub-cultured on HIS-T agar and inoculated into 500 mL tryptone yeast (TY) broth (3.0%
669 tryptone, 2.0% yeast extract, and 0.1% sodium thioglycolate) and grown anaerobically at 37 °C
670 for 10 days. Spores were harvested by centrifugation at 10,000*g* for 20 minutes at 4 °C and
671 washed 5 times with chilled distilled water prior to heat-shocking at 65 °C for 20 minutes and
672 quantified by plating onto HIS-T agar. Spores were adjusted to 10^6 CFU/mL in PBS containing
673 0.05 % Tween-80 in preparation for mouse infections.

674 **Mouse study design**

675 Animal handling and experimentation was performed in accordance with Victorian State
676 Government regulations and approved by the Monash University Animal Ethics Committee
677 (Monash University AEC no. 21731). Male C57BL/6J mice, 6-7 weeks old, were assigned to
678 either a spirulina therapeutic treatment group, positive control (vancomycin-treated), or
679 negative control (wild-type spirulina-treated) group and caged in groups of 5. To induce
680 susceptibility to *C. difficile*, the animals were pre-treated with an antibiotic cocktail in the
681 drinking water containing kanamycin (0.4 mg/mL), gentamicin (0.035 mg/mL), colistin (850
682 U/mL), metronidazole (0.215 mg/mL), vancomycin (0.045 mg/mL), and cefaclor (0.3 mg/mL) for
683 7 days, followed by 4 days of cefaclor (0.3 mg/mL) alone. Starting 1 day prior to infection (day -
684 1), the animals were orally gavaged with 200 µL of treatment once daily for the first two days
685 (peak of infection) and then 100 µL once daily for the remainder of the study. Mice were
686 infected with 10^5 spores/mouse by oral gavage.

687 The spirulina treatments and controls were resuspended in PBS (5% w/v) by mixing up and
688 down using an 18G blunt needle and 1 mL syringe for 2.5 minutes and administered within 10
689 minutes of preparation. Vancomycin was diluted to 6.25 mg/mL prior to administration. On the
690 day of *C. difficile* infection (day 0), antibiotic pre-treatment was ceased, the mice were switched
691 to plain water, and infection was initiated 3 hours after the treatment dose. Mice were
692 monitored daily for signs of infection, including weight loss, and were euthanized upon losing
693 15% body weight, if they reached pre-defined clinical endpoints as required by ethics, or at the
694 end of the study (day 4). As a surrogate assessment of colonization, fecal samples collected at
695 24 hours post-infection and then again at the time of euthanasia were analyzed to enumerate

696 the shedding of *C. difficile* spores. Subjects treated with a spirulina therapeutic cocktail were
697 compared to the cohort administered wild-type spirulina.

698 **Quantification of spore shedding from mouse feces**

699 Fecal pellets were collected 24 hours post-infection and at time of euthanasia, resuspended in
700 PBS (100 mg/mL), heat shocked (30 minutes, 65 °C) and plated for spore enumeration onto HIS
701 agar supplemented with 0.1% (w/v) L-cysteine, 0.1% (w/v) sodium taurocholate, 0.375% (w/v)
702 glucose, 250 µg/mL D-cycloserine, 8 µg/mL cefoxitin, and 10 µg/mL erythromycin.

703 Analysis of colonization data was performed by fitting linear models of $\log_{10}$ cfu/g data per
704 landmark time with treatment as a (potential) explanatory factor. A coefficient for wild-type
705 spirulina describes the mean $\log_{10}$ cfu/g for that treatment, and coefficients for each other
706 treatment describes the difference in mean $\log_{10}$ cfu/g for that treatment relative to wild-type
707 spirulina. Standard errors of estimates were reported, along with t-statistics and 2-tailed p-
708 value corresponding to the t-statistic with α=0.05.

709 **Analysis of clinical outcomes—mouse study**

710 Analysis of maximum weight loss data was performed by fitting linear models of maximum
711 weight loss data with treatment as a (potential) explanatory factor. A coefficient for wild-type
712 spirulina describes the mean maximum weight loss for that treatment, and coefficients for each
713 other treatment describes the difference in mean loss for that treatment relative to wild-type
714 spirulina. Standard errors of estimates were reported, along with t-statistics and 2-tailed p-
715 value corresponding to the t-statistic with α=0.05.

716 Analysis of survival data was performed on tabulated number at risk and number of events at
717 each time. Data was compared for each treatment to wild-type spirulina results and a P value
718 was computed using the log-rank statistic for each comparison.

719 **Hamster study challenge agent preparation and confirmation**

720 *C. difficile* strain R20291 (NAP1/BI/027) spore stock was titered on TCCFA plates after a 30-
721 minute incubation at 65 °C and determined to be 5 x 10^5 cfu/mL in a volume of 5 mL of PBS.
722 This spore stock was diluted to 15,000 spores/50 µL and further diluted in an equal volume of
723 sterile PBS containing 5% sucrose to facilitate administration of 15,000 spores in 100 µL per
724 animal.

725 To verify challenge doses, 100 µL of inoculum were serially diluted (10-fold dilutions) and plated
726 onto TCCFA plates. After incubation of the plates under anaerobic conditions at 37 °C for 48
727 hours, the number of colonies were enumerated, and the doses calculated based on these
728 numbers. The inoculum was measured to be 15,000 cfu.

729 **Hamster study design**

730 Hamsters (Envigo, Indianapolis, IN) were visibly checked upon arrival and allowed to acclimate
731 to their new environment for 2 days. Each animal was given a physical exam and randomly
732 assigned (adjusting only to distribute body weight evenly) to 1 group. They were fed *ad libitum*
733 with sterilized 2018S Teklad Global 18% Rodent Diet (Envigo, Indianapolis, IN) and sterile water
734 provided in standard bottles with sippers during the study. To sensitize the animals to *C. difficile*
735 infection, clindamycin, 15 mg/mL in saline, was administered intraperitoneally at 30 mg/kg,
736 once a day, for 3 consecutive days. During clindamycin treatment, cage bottoms were changed

737 daily for 3 consecutive days beginning on the first day to prevent bacterial recolonization from

738 coprophagy.

ACKNOWLEDGEMENTS

We thank Charles Shoemaker, George McDonald, and Fred Cross for help, discussion, and advice. We thank Meagan James and other members of the Lyras laboratory for help with the mouse studies. For the hamster challenge studies Lumen Bioscience has utilized the non-clinical and pre-clinical services program offered by the National Institute of Allergy and Infectious Diseases, especially support from Sangun Lee, Christian Gonzalez and Ryan Ranallo.

747 **REFERENCES**
748

749 1. Knight, D. R., Elliott, B., Chang, B. J., Perkins, T. T. & Riley, T. V. Diversity and Evolution in the
750 Genome of *Clostridium difficile*. *Clinical Microbiology Reviews* 28, 721–741 (2015).

751 2. Balsells, E. *et al.* Global burden of *Clostridium difficile* infections: a systematic review and
752 meta-analysis. *Journal of Global Health* 9, 010407 (2019).

753 3. Guh, A. Y. *et al.* Trends in U.S. Burden of *Clostridioides difficile* Infection and Outcomes. *N.*
754 *Engl. J. Med.* 382, 1320–1330 (2020).

755 4. Salavert, M. *et al.* Cost-effectiveness analysis of bezlotoxumab added to standard of care
756 versus standard of care alone for the prevention of recurrent *Clostridium difficile* Infection in
757 High-Risk Patients in Spain *Adv. Ther* (2018) doi:doi.org/10.1007/s12325-018-0813-y.

758 5. Seal, D. *et al.* Treatment of relapsing *Clostridium difficile* diarrhoea by administration of a
759 non-toxigenic strain. *Eur J Clin Microbiol* 6, 51–53 (1987).

760 6. Kuehne, S. A. *et al.* The role of toxin A and toxin B in *Clostridium difficile* infection. *Nature*
761 467, 711–713 (2010).

762 7. Lyras, D. *et al.* Toxin B is essential for virulence of *Clostridium difficile*. *Nature* 458, 1176–
763 1179 (2009).

764 8. Chen, K. *et al.* A probiotic yeast-based immunotherapy against *Clostridioides difficile*
765 infection. *Sci Transl Med* 12, eaax4905 (2020).

766 9. Tao, L. *et al.* Frizzled proteins are colonic epithelial receptors for *C. difficile* toxin B. *Nature*
767 538, 350–355 (2016).

768 10. Henkel, D. *et al.* Receptor Binding Domains of TcdB from *Clostridioides difficile* for
769 Chondroitin Sulfate Proteoglycan-4 and Frizzled Proteins Are Functionally Independent and
770 Additive. *Toxins (Basel)* 12, 736 (2020).

771 11. Qa'Dan, M., Spyres, L. M. & Ballard, J. D. pH-induced conformational changes in *Clostridium*
772 *difficile* toxin B. *Infection and Immunity* 68, 2470–2474 (2000).

773 12. Reineke, J. *et al.* Autocatalytic cleavage of *Clostridium difficile* toxin B. *Nature* 446, 415–419
774 (2007).

775 13. Sehr, P. *et al.* Glucosylation and ADP ribosylation of rho proteins: effects on nucleotide
776 binding, GTPase activity, and effector coupling. *Biochemistry* 37, 5296–5304 (1998).

777 14. Just, I. *et al.* Glucosylation of Rho proteins by *Clostridium difficile* toxin B. *Nature* 375, 500–
778 503 (1995).

779 15. Aelst, L. V. & Symons, M. Role of Rho family GTPases in epithelial morphogenesis. *Genes &*
780 *Development* 16, 1032–1054 (2002).

781 16. Schlegel, N., Meir, M., Spindler, V., Germer, C.-T. & Waschke, J. Differential role of Rho
782 GTPases in intestinal epithelial barrier regulation in vitro. *J Cell Physiol* 226, 1196–1203 (2011).

783 17. Pradhan, R., Ngo, P. A., Martínez-Sánchez, L. D., Neurath, M. F. & López-Posadas, R. Rho
784 GTPases as Key Molecular Players within Intestinal Mucosa and GI Diseases. *Cells* 10, 66 (2021).

785 18. Carter, G. P. *et al.* Defining the Roles of TcdA and TcdB in Localized Gastrointestinal Disease,
786 Systemic Organ Damage, and the Host Response during *Clostridium difficile* Infections. *mBio* 6,
787 e00551 (2015).

788 19. Mileto, S. J. *et al.* Clostridioides difficile infection damages colonic stem cells via TcdB,
789 impairing epithelial repair and recovery from disease. *Proceedings of the National Academy of*
790 *Sciences* 117, 8064–8073 (2020).

791 20. Bella, S. D., Ascenzi, P., Siarakas, S., Petrosillo, N. & Masi, A. di. *Clostridium difficile* Toxins A
792 and B: Insights into Pathogenic Properties and Extraintestinal Effects. *Toxins (Basel)* 8, 134–25
793 (2016).

794 21. Hutton, M. L. *et al.* Bovine antibodies targeting primary and recurrent *Clostridium difficile*
795 disease are a potent antibiotic alternative. *Sci. Rep.* 7, 16020–13 (2017).

796 22. Steele, J., Mukherjee, J., Parry, N. & Tzipori, S. Antibody Against TcdB, but Not TcdA,
797 Prevents Development of Gastrointestinal and Systemic *Clostridium difficile* Disease. *J. Infect.*
798 *Dis.* 207, 323–330 (2012).

799 23. Wilcox, M. H. *et al.* Bezlotoxumab for Prevention of Recurrent *Clostridium difficile* Infection.
800 *N. Engl. J. Med.* 376, 305–317 (2017).

801 24. Dieterle, M. G., Rao, K. & Young, V. B. Novel therapies and preventative strategies for
802 primary and recurrent *Clostridium difficile* infections. *Annals of the New York Academy of*
803 *Sciences* 1435, 110–138 (2019).

804 25. Song, J. H. & Kim, Y.-S. Recurrent *Clostridium difficile* Infection: Risk Factors, Treatment, and
805 Prevention. *Gut Liver* 13, 16–24 (2019).

806 26. Singh, T. *et al.* Updates in Treatment of Recurrent *Clostridium difficile* Infection. *J Clin Med*
807 *Res* 11, 465–471 (2019).

808 27. Pruss, K. M. & Sonnenburg, J. L. *C. difficile* exploits a host metabolite produced during toxin-
809 mediated disease. *Nature* 593, 261–265 (2021).

810 28. Yang, Z. *et al.* A novel multivalent, single-domain antibody targeting TcdA and TcdB prevents
811 fulminant *Clostridium difficile* infection in mice. *J. Infect. Dis.* 210, 964–972 (2014).

812 29. Schmidt, D. J. *et al.* A Tetraspecific VHH-Based Neutralizing Antibody Modifies Disease
813 Outcome in Three Animal Models of Clostridium difficile Infection. *Clinical and Vaccine*
814 *Immunology* 23, 774–784 (2016).

815 30. Roberts, A. K. *et al.* A Novel, Orally Delivered Antibody Therapy and Its Potential to Prevent
816 *Clostridioides difficile* Infection in Pre-clinical Models. *Front Microbiol* 11, 578903 (2020).

817 31. Babcock, G. J. *et al.* Human Monoclonal Antibodies Directed against Toxins A and B Prevent
818 *Clostridium difficile*-Induced Mortality in Hamsters. *Infection and Immunity* 74, 6339–6347
819 (2006).

820 32. Sponseller, J. K. *et al.* Hyperimmune Bovine Colostrum as a Novel Therapy to Combat
821 *Clostridium difficile* Infection. *J. Infect. Dis.* 5, 549–8 (2014).

822 33. Mansfield, M. J. *et al.* Phylogenomics of 8,839 *Clostridioides difficile* genomes reveals
823 recombination-driven evolution and diversification of toxin A and B. *PLoS Pathog* 16, e1009181
824 (2020).

825 34. Bartlett, J. G. Bezlotoxumab — A New Agent for *Clostridium difficile* Infection. *N. Engl. J.*
826 *Med.* 376, 381–382 (2017).

827 35. Dissel, J. T. van *et al.* Bovine antibody-enriched whey to aid in the prevention of a relapse of
828 *Clostridium difficile*-associated diarrhoea: preclinical and preliminary clinical data. *J Med*
829 *Microbiol* 54, 197–205 (2005).

830 36. Numan, S. C., Veldkamp, P., Kuijper, E. J., Berg, R. J. van den & Dissel, J. T. van. Clostridium
831 difficile-associated diarrhoea: bovine anti-*Clostridium difficile* whey protein to help aid the
832 prevention of relapses. *Gut* 56, 888 (2007).

833 37. Mattila, E. *et al.* A randomized, double-blind study comparing *Clostridium difficile* immune
834 whey and metronidazole for recurrent Clostridium difficile-associated diarrhoea: Efficacy and
835 safety data of a prematurely interrupted trial. *Scand J Infect Dis* 40, 702–708 (2009).

836 38. McGovern, B. H. *et al.* SER-109, an Investigational Microbiome Drug to Reduce Recurrence
837 after *Clostridioides difficile* infection: Lessons Learned from a Phase 2 Trial. *Clin Infect Dis* 313,
838 1719 (2020).

839 39. Ghose, C. & Kelly, C. P. The Prospect for Vaccines to Prevent *Clostridium difficile* Infection.
840 *Infectious Disease Clinics of North America* 29, 145–162 (2015).

841 40. Bruyn, G. de *et al.* Safety, immunogenicity, and efficacy of a *Clostridioides difficile* toxoid
842 vaccine candidate: a phase 3 multicentre, observer-blind, randomised, controlled trial. *The*
843 *Lancet Infectious Diseases* 21, 252–262 (2021).

844 41. Chen, P. *et al.* Structure of the full-length Clostridium difficile toxin B. *Nat Struct Mol Biol* 26,
845 712–719 (2019).

846 42. Wang, Q., Euler, C. W., Delaune, A. & Fischetti, V. A. Using a Novel Lysin To Help Control
847 *Clostridium difficile* Infections. *Antimicrobial Agents and Chemotherapy* 59, 7447–7457 (2015).

848 43. Fischetti, V. A. Bacteriophage lysins as effective antibacterials. *Current Opinion in*
849 *Microbiology* 11, 393–400 (2008).

850 44. Peng, Z. *et al.* A Novel Bacteriophage Lysin-Human Defensin Fusion Protein Is Effective in
851 Treatment of *Clostridioides difficile* Infection in Mice. *Front. Microbio.* 9, 3234 (2018).

852 45. Jester, B. *et al.* Expression and manufacturing of protein therapeutics in spirulina. *bioRxiv*
853 2021.01.25.427910 (2021) doi:10.1101/2021.01.25.427910.

854 46. Raran-Kurussi, S. & Waugh, D. S. The Ability to Enhance the Solubility of Its Fusion Partners
855 Is an Intrinsic Property of Maltose-Binding Protein but Their Folding Is Either Spontaneous or
856 Chaperone-Mediated. *Plos One* 7, e49589 (2012).

857 47. Hanoune, J. & Defer, N. Regulation and role of adenylyl cyclase isoforms. *Annu. Rev.*
858 *Pharmacol. Toxicol.* 41, 145–174 (2001).

859 48. Burgers, P. P. *et al.* Structure of smAKAP and its regulation by PKA-mediated
860 phosphorylation. *FEBS J* 283, 2132–2148 (2016).

861 49. Ryder, A. B. *et al.* Assessment of *Clostridium difficile* Infections by Quantitative Detection of
862 tcdB Toxin by Use of a Real-Time Cell Analysis System. *J Clin Microbiol* 48, 4129–4134 (2010).

863 50. Pollock, N. R. Ultrasensitive Detection and Quantification of Toxins for Optimized Diagnosis
864 of *Clostridium difficile* Infection. *Journal of Clinical Microbiology* 54, 259–264 (2016).

865 51. Shen, E. *et al.* Subtyping analysis reveals new variants and accelerated evolution of
866 Clostridioides difficile toxin B. *Commun Biology* 3, 347 (2020).

867 52. Alonso, C. D. *et al.* Ultrasensitive and quantitative toxin measurement correlates with
868 baseline severity, severe outcomes, and recurrence among hospitalized patients with
869 *Clostridioides difficile* infection. *Clin Infect Dis* ciab826- (2021) doi:10.1093/cid/ciab826.

870 53. Tickler, I. A. *et al.* Changes in molecular epidemiology and antimicrobial resistance profiles
871 of *Clostridioides (Clostridium) difficile* strains in the United States between 2011 and 2017.
872 *Anaerobe* 60, 102050 (2019).

873 54. Li, Z. *et al.* Ribotype Classification of *Clostridioides difficile* Isolates Is Not Predictive of the
874 Amino Acid Sequence Diversity of the Toxin Virulence Factors TcdA and TcdB. *Front Microbiol*
875 11, 1310 (2020).

876 55. Chou, T. C. & Talaly, P. A simple generalized equation for the analysis of multiple inhibitions
877 of Michaelis-Menten kinetic systems. *J. Biol. Chem.* 252, 6438–6442 (1977).

878 56. Einav, T. & Bloom, J. D. When two are better than one: Modeling the mechanisms of
879 antibody mixtures. *Plos Comput Biol* 16, e1007830 (2020).

880 57. Gilchuk, P. *et al.* Analysis of a Therapeutic Antibody Cocktail Reveals Determinants for
881 Cooperative and Broad Ebolavirus Neutralization. *Immunity* 52, 388-403.e12 (2020).

882 58. Mulangu, S. *et al.* A Randomized, Controlled Trial of Ebola Virus Disease Therapeutics. *New*
883 *Engl J Med* 381, 2293–2303 (2019).

884 59. Weinreich, D. M. *et al.* REGN-COV2, a Neutralizing Antibody Cocktail, in Outpatients with
885 Covid-19. *New Engl J Medicine* 384, NEJMoa2035002 (2020).

886 60. Shah, D. K. & Betts, A. M. Antibody biodistribution coefficients: inferring tissue
887 concentrations of monoclonal antibodies based on the plasma concentrations in several
888 preclinical species and human. *mAbs* 5, 297–305 (2013).

889 61. Mudie, D. M. *et al.* Quantification of Gastrointestinal Liquid Volumes and Distribution
890 Following a 240 mL Dose of Water in the Fasted State. *Mol. Pharmaceutics* 11, 3039–3047
891 (2014).

892 62. Schiller, C. *et al.* Intestinal fluid volumes and transit of dosage forms as assessed by
893 magnetic resonance imaging. *Aliment Pharmacol Ther* 22, 971–979 (2005).

894 63. Gerding, D. N., Johnson, S., Rupnik, M. & Aktories, K. *Clostridium difficile* binary toxin CDT.
895 *Gut Microbes* 5, 15–27 (2014).

896 64. Studier, F. W. Protein production by auto-induction in high-density shaking cultures. *Protein*
897 *Expres Purif* 41, 207–234 (2005).

898 65. Moré, J. J. Numerical Analysis. *Lect Notes Math* 105–116 (1978) doi:10.1007/bfb0067700.

899 66. *Akaike information criterion statistics*. vol. 29 (reidel, 1987).

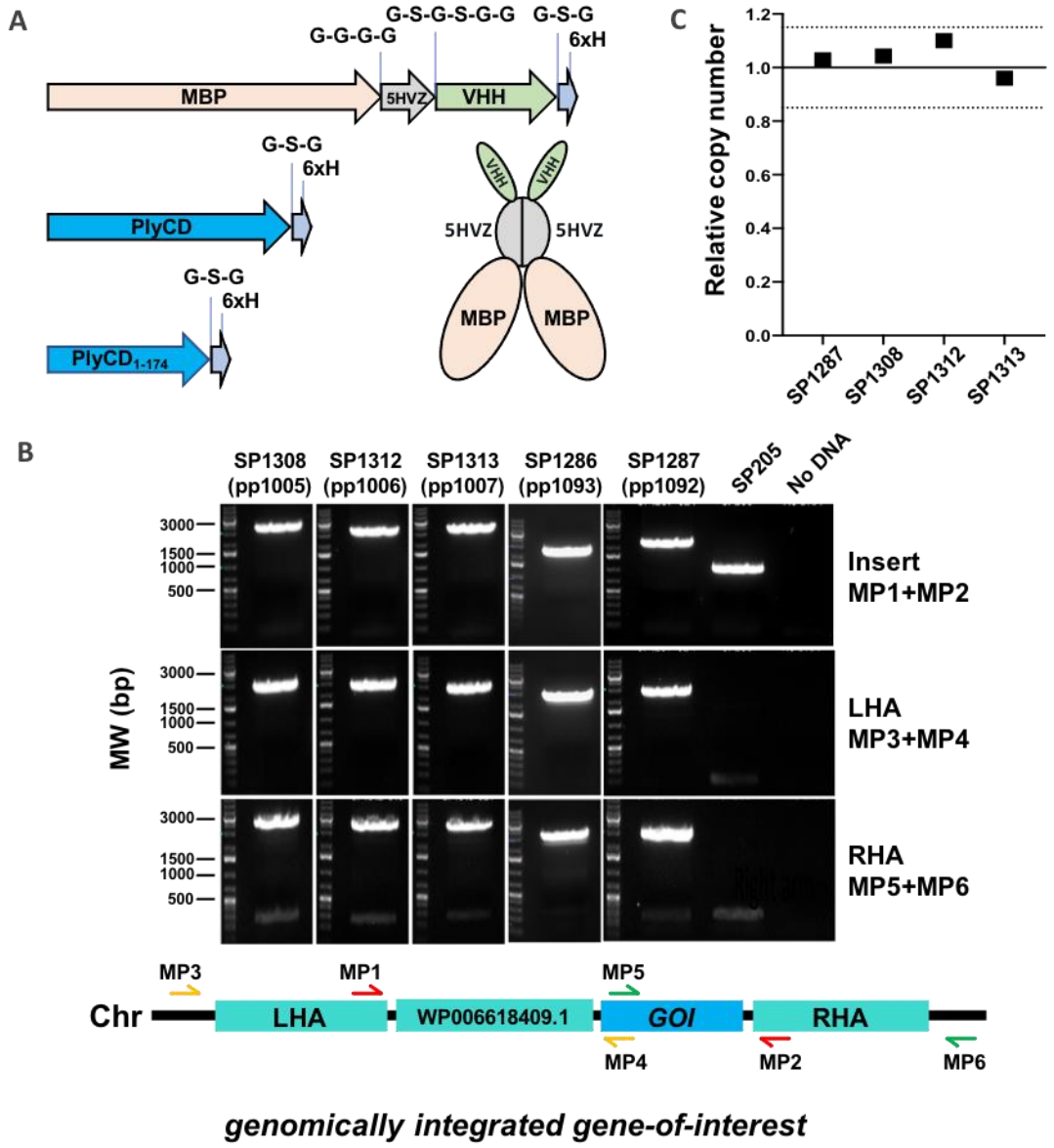

Figure 1. Spirulina strain engineering and characterization. A) Diagram of modified anti-*C. difficile* TdcB VHHs 5D, E3, 7F, PlyCD, PlyCD$_{1-174}$, and 5HVZ-mediated dimer formation. B) A schematic diagram of the genomic integration locus (WP_006618409.1). PCR was performed with indicated primers to analyze the segregation and specificity of integration for each strain. PCR products with primers MP1/MP2 showed bands of predicted sizes in all strains, and absence of the parental alleles, suggesting the segregation to homozygosity was complete. The primer pairs for amplification of the left homology arm (LHA) and right homology arm (RHA) include one priming site (MP3 and MP6) that is only present in the spirulina genome at the target locus and absent from the donor plasmid. PCR amplification of the LHA and RHA with MP3/MP4 and MP5/MP6, respectively, demonstrated that genomic integration was site-specific. The DNA sequences from all PCR products were verified to match expectations. C) Copy numbers of the genes of interest (GOIs) were determined with next-generation

914 sequencing by comparing reads of the GOIs to ten randomly selected native spirulina genes.
915 Dotted line indicates range in which the relative copy numbers were considered equivalent to
916 one.
917

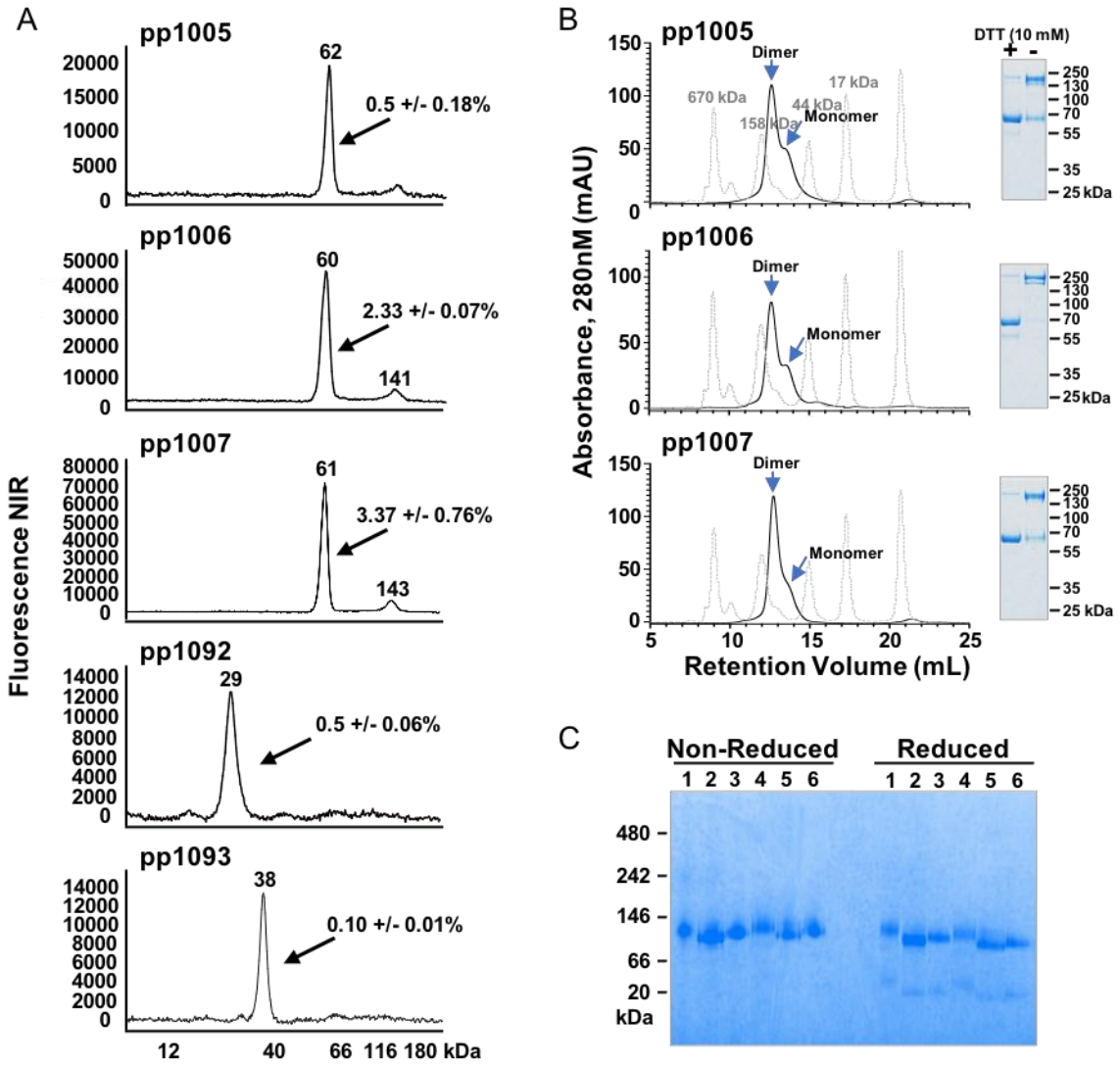

Figure 2. Characterization of spirulina-expressed anti-TcdB VHHs and lysins. A) Chromatograms of pp1005, pp1006, pp1007, pp1092, and pp1093 extracted from spirulina biomass and detected under reducing conditions using a capillary electrophoresis-based immunoassay. Soluble protein, as a percentage of washed dry weight, is indicated on each graph. B) Spirulina expressed and purified pp1005, pp1006, and pp1007 in aqueous solution (PBS, pH 7.4) assayed on a Superdex 200 10/300 GL FPLC column. Grey peaks correspond to molecular size standards. The monomeric and dimeric portions of the VHHs are indicated. Disulfide bond formation between monomers was assessed using denaturing gel electrophoresis under non-reducing and reducing (50 mM DTT) conditions. C) Native gel electrophoresis analysis of pp1005 (1, 4), pp1006 (2, 5), and pp1007 (3, 6) under non-reducing or reducing (50 mM DTT) conditions. In the presence of reducing agent the dimeric state of the VHHs was mostly preserved.

A

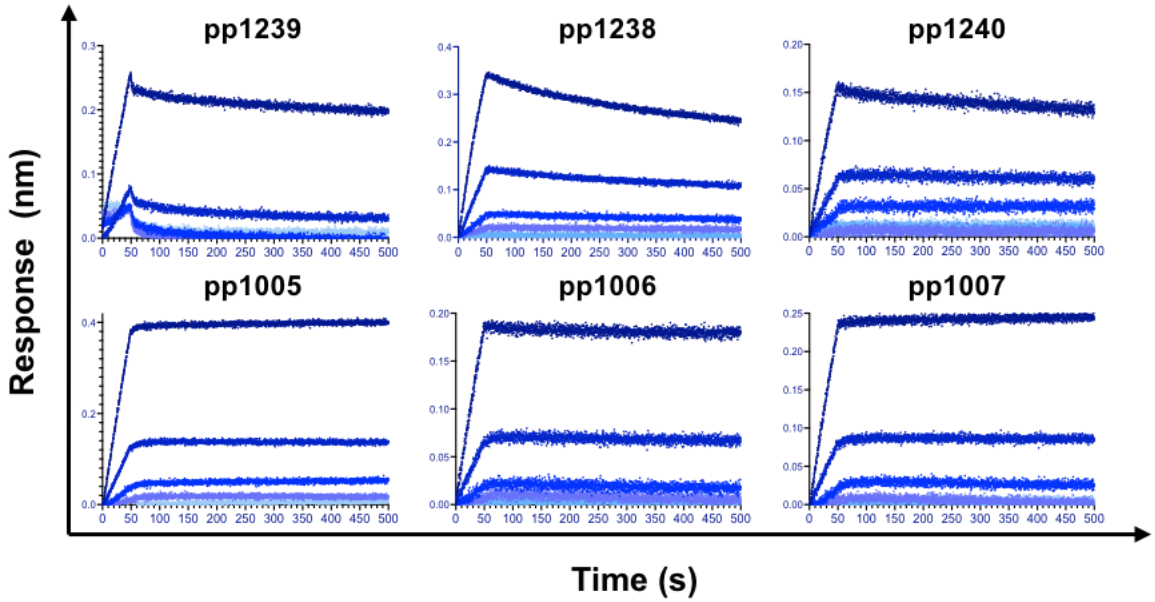

B

Sample ID	K_D (nM)	k_a (1/Ms)	k_d (1/s)
pp1239 (M)	2.56 (0.02)	1.64E+05 (0.12)	4.20E-04 (0.13)
pp1005 (D)	0.002 (0)	1.16E+05 (0.11)	2.59E-07 (0)
pp1238 (M)	4.85 (0.06)	1.45E+05 (0.02)	7.02E-04 (0.02)
pp1006 (D)	0.03 (0)	7.48E+04 (1.68)	2.57E-06 (0)
pp1240 (M)	2.09 (0.06)	1.26E+05 (0.04)	2.63E-04 (0.03)
pp1007 (D)	0.58 (0.07)	1.54E+05 (0.17)	8.97E-05 (0.30)

Figure 3. Binding affinities and toxin neutralizing activity of TcdB VHHs. A) BLI binding sensorgrams for analysis of binding kinetic for anti-TcdB VHHs as monomers (pp1239, pp1238, and pp1240) and dimers (pp1005, pp1006, and pp1007). B) The rate constants k_a and k_d were calculated from concentration-dependent responses. The apparent equilibrium binding constant (K_D) for each was determined from the rate of association (k_a), and rate of dissociation (k_d). Values of K_D, k_a and k_d are indicated in the table (M, monomer; D, dimer).

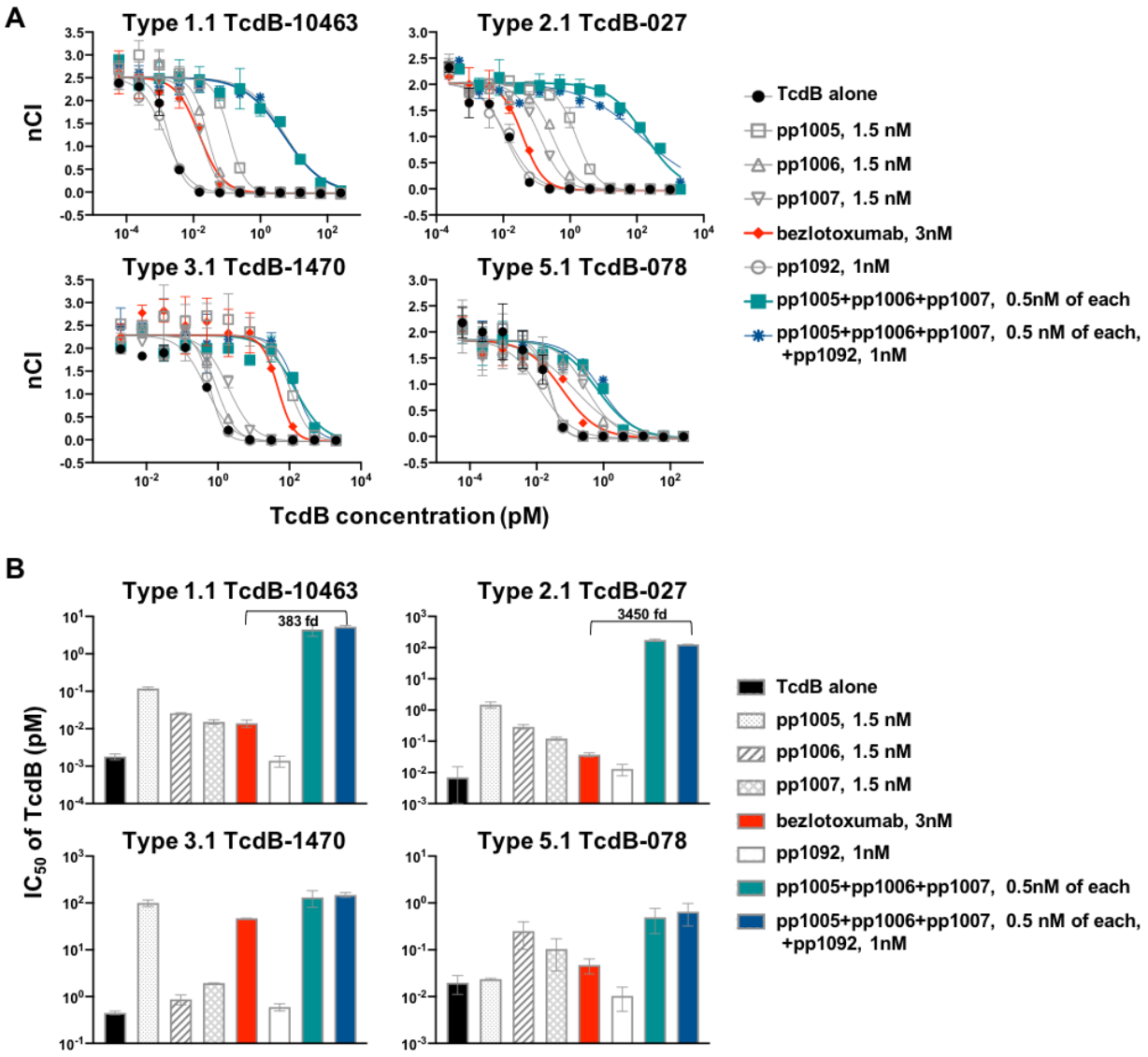

Figure 4. Comparative neutralization of the five major TcdB types by LMN-201 and bezlotoxumab. A) Neutralizing activity of pp1005, pp1006, pp1007, and the triple cocktail on toxin types 1.1, 2.1, 3.1 and 5.1. 1.5 nM of each dimeric VHH or the cocktail of all three dimeric VHHs (0.5 nM of each) was tested against serially diluted TcdB with Vero cells on the RTCA system. As comparison, 3 nM of bezlotoxumab was similarly evaluated. To rule out interference, the effect of 1 nM lysin on VHH cocktail efficacy was assessed. B) IC_{50} of TcdB under treatment was calculated from the data shown in A and compared.

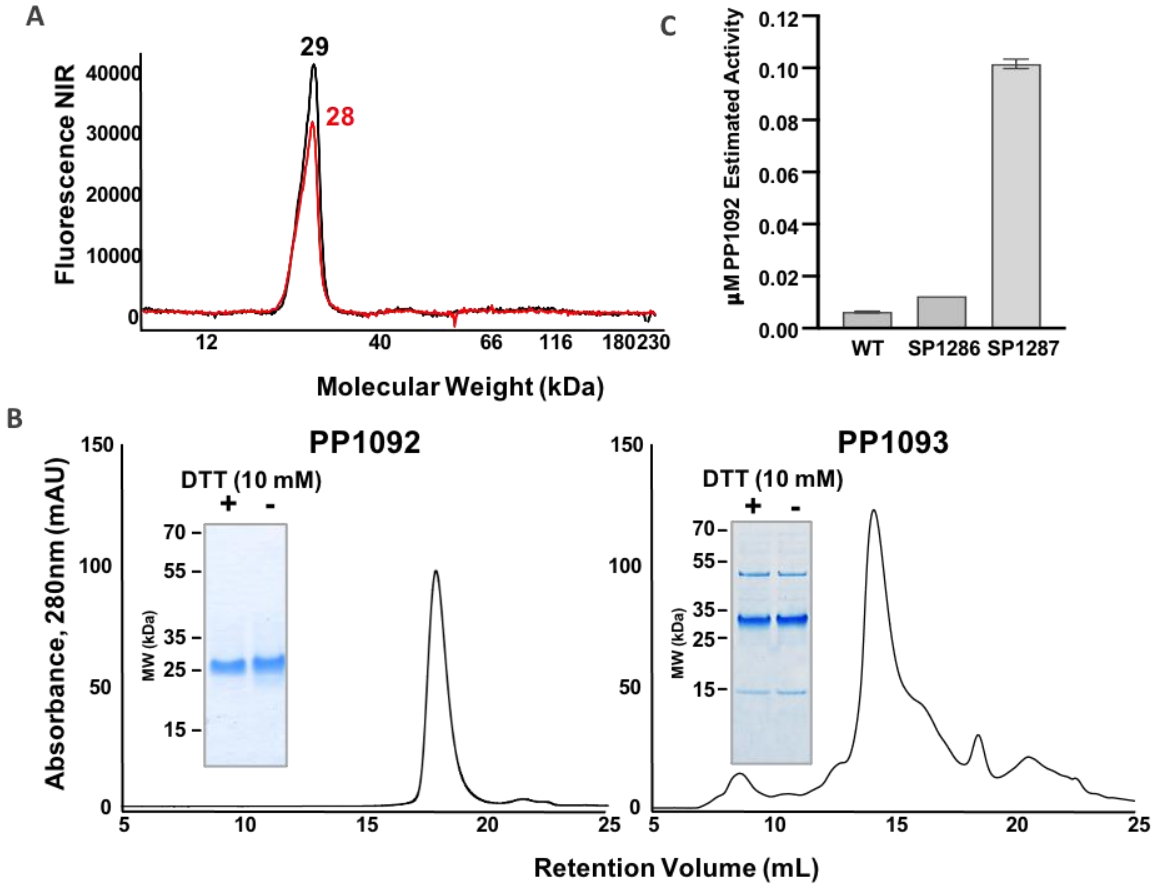

Figure 5. Characterization of spirulina-expressed anti-*C. difficile* lysin. A) A chromatogram of pp1092 after total protein extraction (black) and soluble protein extraction (red). More than 75% of the lysin protein is soluble. B) Spirulina-expressed, purified lysins, pp1092 and pp1093, in aqueous solution (1xPBS, pH 7.4) evaluated by size-exclusion chromatography (Superdex 200 10/300 GL FPLC column). Purified protein samples were also assessed using denaturing gel electrophoresis under non-reducing and reducing (50 mM DTT) conditions. C) Activity of spirulina extracts (wild-type (WT) expressing no lysin, SP1286 expressing pp1093, and SP1287 expressing pp1092) prepared at 2 mg/mL were compared by measuring the time to reduce turbidity of living *B. subtilis* SL4 cultures by 50%.

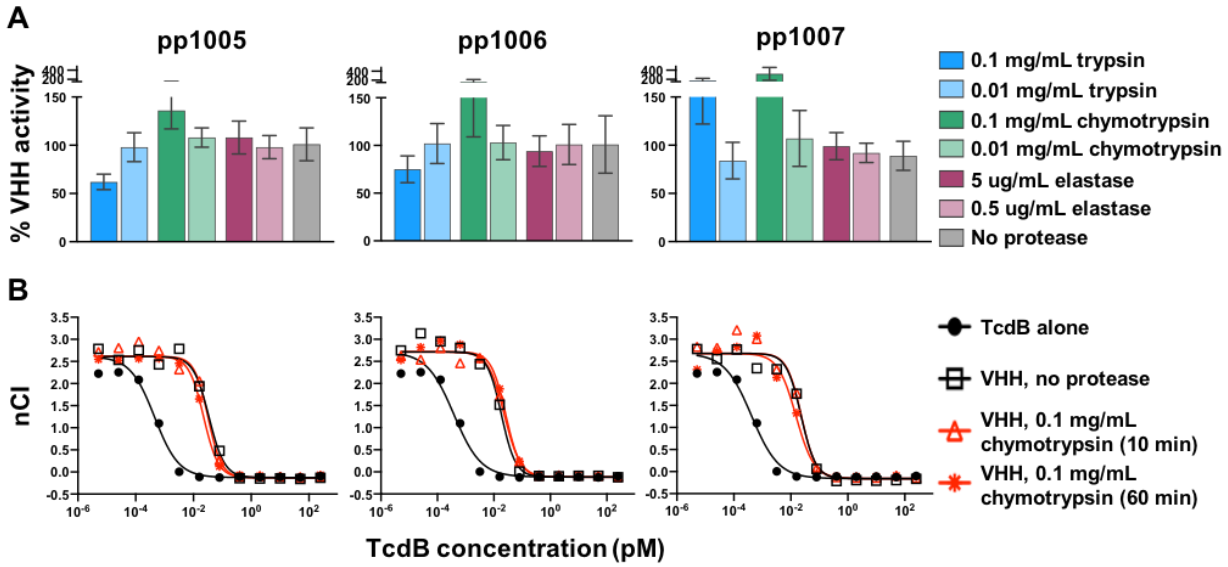

Figure 6. Stability of anti-TcdB VHHs to gastrointestinal proteases. A) The percentage of TcdB-binding activity of pp1005, pp1006, and pp1007 measured by ELISA after digestion with trypsin (T), chymotrypsin (C), and elastase (E). Two concentrations of each protease were tested to simulate either "fed" (higher concentration) or "fasted" (lower concentration) conditions. Data represent the average of six independent replicates, the error bars representing the standard deviation. B) TcdB-neutralizing activity of protease digested pp1005, pp1006, and pp1007. VHH homodimers treated with chymotrypsin for either 10 or 60 minutes were compared in a cell-rounding assay with the corresponding undigested protein. Each was diluted to a fixed concentration (pp1005 was 0.05 nM, pp1006 was 5 nM, and pp1007 was 5 nM) and incubated with serially diluted TcdB-10463. Each mixture was assayed for its effect on cell adhesion. After digestion all exhibited neutralizing activities similar to undigested controls.

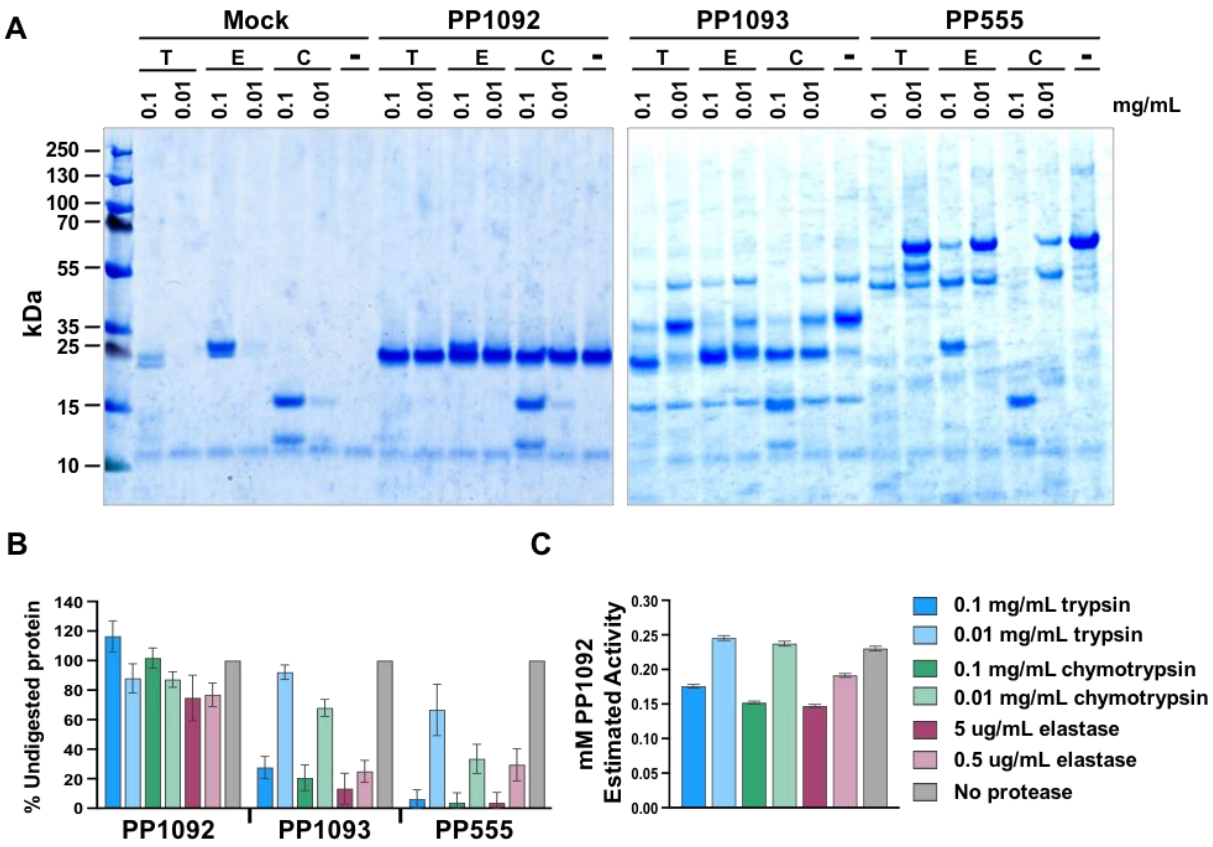

Figure 7. Stability of anti-*C. difficile* lysin to gastrointestinal proteases. A) Full-length lysin (pp1093, 37 kDa), its catalytic subdomain (pp1092, 25 kDa), and a protease sensitive VHH (pp555, 55 kDa) were digested with trypsin (T), chymotrypsin (C), and elastase (E) at pH 6.4 for 1 hour at 37 °C, quenched with protease inhibitors, the products separated by size using PAGE, and peptides visualized by Coomassie staining. Mock digestions without target proteins were performed to visualize the contribution by the proteases and quenching reagents. B) The image in A (representative of six independent digestions) was quantified by densitometry with error expressed as SEM. C) Activities of pp1092 digests were measured by determining the time to reduce the turbidity of a culture of live *B. subtilis* SL4 by 50%. This value was then plotted against a standard curve of undigested reference lysin to determine the activities of the digested samples compared to undigested reference lysin. The dotted line represents the activity of lysin when undigested. Error bars represent the standard error calculated from three technical replicates.

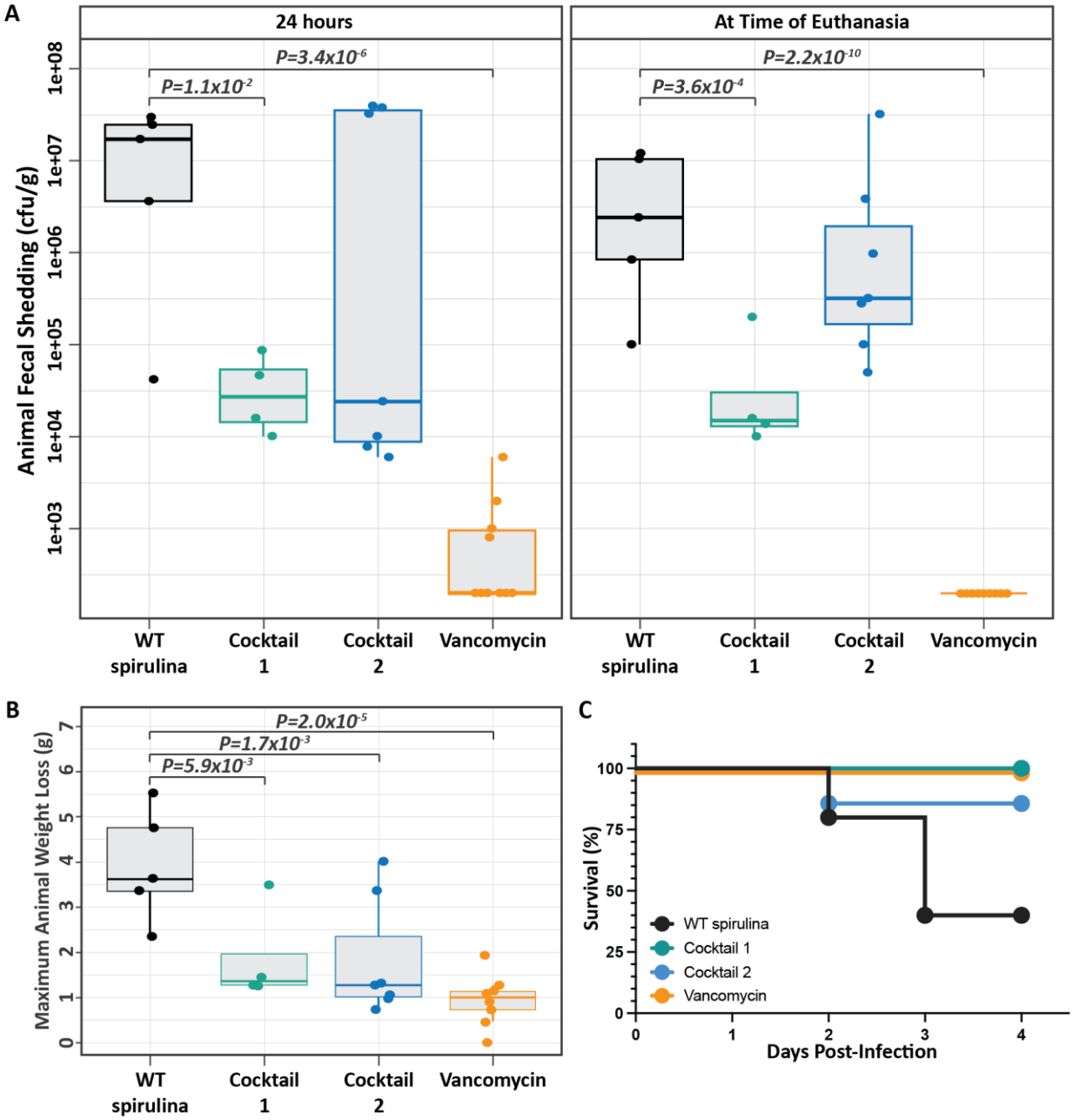

Figure 8. Mouse challenge study. Shown are A) fecal spore counts 24 hours after infection and at the time of euthanasia; B) maximum weight loss for individuals in each group; and C) Kaplan-Meier representation of survival. Individuals were euthanized upon losing ≥15% of their initial weight. Individuals in panels A and B are represented as a point and the group median, interquartile range (IQR) and 1.5*IQR as boxplots. A) Log_{10} fecal shedding data were fit with a linear model with group as a predictor per time point. Treatment group is a significant predictor ($p<0.05$) of shedding relative to the wild-type spirulina group (control/intercept) for Cocktail 1 and vancomycin. Cocktail 2 fails significance testing ($p\sim0.1$ and $p\sim0.25$). Statistic reports the t ratio based on a Student t reference distribution, and p-value reports the two-tailed p-value corresponding to the t ratio based on the Student t reference distribution. B) Maximum animal

1007 weight loss was fit with a linear model with treatment as predictors of weight loss. Treatment
1008 group is a significant predictor ($p<0.05$) of animal weight loss relative to the wild-type spirulina
1009 group (control). C) Kaplan-Meier survival curves for mice infected with 10^5 *C. difficile* spores and
1010 treated with vancomycin (orange, n=10), wild-type spirulina (black, n=5), spirulina therapeutic
1011 Cocktail 1 (teal, n=5) or Cocktail 2 (blue, n=7). Survival rates were compared to treatment with
1012 wild-type spirulina by log-rank test. Significance was observed with vancomycin treatment
1013 ($p=0.0068$), borderline significance was observed with spirulina Cocktail 1 ($p=0.080$) and
1014 Cocktail 2 ($p=0.14$) treatment.
1015

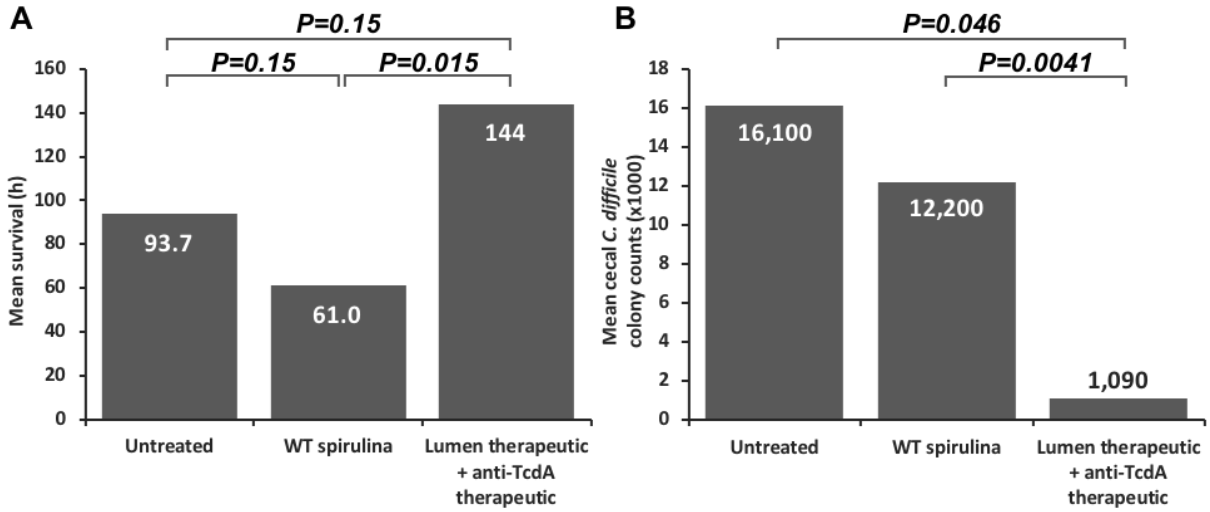

1016
1017
1018 **Figure 9.** Hamster challenge trial. A) The Lumen therapeutic prolonged survival times when
1019 compared to the untreated and group administered wild-type spirulina. Clindamycin-treated
1020 Golden Syrian hamsters were administered phosphate-buffered saline, wild-type spirulina, or
1021 the Lumen therapeutic two times a day starting one day before infection with *C. difficile*
1022 (15,000 spores) and continuing until they reached their humane endpoints or the end of the
1023 study (14 days post-infection). The mean survival times were compared using a Mann-Whitney
1024 test with continuity correction, 90% confidence level, one-sided test. B) Lumen therapeutic
1025 decreased *C. difficile* cecal colonization. Cecal contents were collected after animals reached
1026 their humane endpoints or the termination date. *C. difficile* colony counts were quantified by
1027 comparing RT-PCR measurements of extracted DNA from these samples as compared to a
1028 standard curve generated by DNA extracted from vegetative *C. difficile* cells. Fewer *C. difficile*
1029 cells colonized the cecum in hamsters treated with the Lumen therapeutic than in wild-type
1030 spirulina-treated or untreated groups. Wilcoxon rank sum test (Mann-Whiney test) with
1031 continuity correction, 90% confidence level, one-sided test.
1032

Parameter	Estimate	Std. error	p-value	2.5% CI	97.5% CI
TcdB IC_{50} (fM)	1.268	6.57E-05	2.24E-52	0.001138	0.001397
$Hill^{TcdB}$	1.495	0.07091	1.35E-58	1.355	1.634
EC_{50}^{pp1005} (pM)	21.44	0.002423	1.28E-16	0.01667	0.02622
$Hill^{pp1005}$ (-)	1.813	0.1245	1.12E-35	1.567	2.058
E_{max}^{pp1005} (fold)	45.25	3.076	3.20E-36	39.2	51.31
EC_{50}^{pp1006} (pM)	54.13	0.003761	4.25E-35	0.04673	0.06154
EC_{50}^{pp1007} (pM)	69.26	0.004852	1.11E-34	0.05971	0.07882
Bottom (assay units)	-0.01326	0.006172	0.0326	-0.02541	-0.001107
Top (assay units)	0.9289	0.01145	3.39E-189	0.9064	0.9515

Table 1. EC_{50} values for pp1005, pp1006, and pp1007. *Independent* model estimates from analysis of the overall data set. TcdB1 acts as an inhibitor of cellular adhesion with femtomolar potency (IC_{50}, H). pp1005, pp1006, and pp1007 act to inhibit TcdB1 activity, shifting TcdB1 potency 2-fold at 10's of picomolar potency (EC_{50}^{pp1005}, EC_{50}^{pp1006}, EC_{50}^{pp1007}). pp1005 activity saturates at around 50-fold (E_{max}^{pp1005}, $Hill^{pp1005}$) while the somewhat less potent pp1006 and pp1007 do not saturate.